

# Learning the hub graphical Lasso model with the structured sparsity via an efficient algorithm

Chengjing Wang\*    Peipei Tang<sup>†</sup>    Wenling He<sup>‡</sup>    Meixia Lin<sup>§</sup>

August 21, 2023

## Abstract

Graphical models have exhibited their performance in numerous tasks ranging from biological analysis to recommender systems. However, graphical models with hub nodes are computationally difficult to fit, particularly when the dimension of the data is large. To efficiently estimate the hub graphical models, we introduce a two-phase algorithm. The proposed algorithm first generates a good initial point via a dual alternating direction method of multipliers (ADMM), and then warm starts a semismooth Newton (SSN) based augmented Lagrangian method (ALM) to compute a solution that is accurate enough for practical tasks. The sparsity structure of the generalized Jacobian ensures that the algorithm can obtain a nice solution very efficiently. Comprehensive experiments on both synthetic data and real data show that it obviously outperforms the existing state-of-the-art algorithms. In particular, in some high dimensional tasks, it can save more than 70% of the execution time, meanwhile still achieves a high-quality estimation.

**Keywords:** hub graphical Lasso, structured sparsity, augmented Lagrangian method, semismooth Newton method

**AMS subject classification:** 65K05, 90C06, 90C25, 90C90

## 1 Introduction

Graphical models have been widely adopted to characterize relationships of data variables in various applications, such as gene finding, medical diagnosis, modeling of protein structures, and so on. To encode conditional dependence relationships among a set of variables, the Gaussian graphical model is employed to estimate the precision matrix  $\Theta = \Sigma^{-1}$  of the data distribution,

---

\*School of Mathematics, Southwest Jiaotong University, No.999, Xian Road, West Park, High-tech Zone, Chengdu 611756, China (Email: renaissancewang@hotmail.com).

<sup>†</sup>**Corresponding author**, School of Computer and Computing Science, Hangzhou City University, Hangzhou 310015, China (Email: tangpp@hzcu.edu.cn).

<sup>‡</sup>School of Mathematics, Southwest Jiaotong University, No.999, Xian Road, West Park, High-tech Zone, Chengdu 611756, China (Email: 1165649932@qq.com).

<sup>§</sup>Engineering Systems and Design, Singapore University of Technology and Design, Singapore. This author's research is supported by The Singapore University of Technology and Design under MOE Tier 1 Grant SKI 2021.02.08. (Email:meixia.lin@sutd.edu.sg).

where  $\Sigma$  is the corresponding covariance matrix, and then the sparsity pattern of  $\Theta$  is used to determine the conditional independence graph [8]. In particular, each variable in the Gaussian graphical model represents a node in a graph, and an edge will link two nodes if the corresponding entry of the precision matrix  $\Theta$  is non-zero. A series of variants of Gaussian graphical model have been designed to satisfy the different requirements of practical tasks, one may refer to [43], [31], [20], [10], [27], [21], [38], [28], [36], and [6], to name but a few.

Among these studies, one interesting problem is to construct a graph with *hubs*, i.e., learning a graphical model that contains a few special nodes, which are *densely-connected* to several other nodes. Such kind of graph is universal in the real world. For instance, in the social network of Twitter, only a few users (e.g., famous actors) have a large number of followers and their tweets have strong influence, while most users do not [15]. A more typical example is the gene-regulatory networks, which are generally thought to approximate a hierarchical scale-free network topology [3], i.e., the number of edges follows a power-law distribution. In addition, one can refer to [1], [18], and [14] for more examples.

To model a graph with hubs, Tan et al. [37] proposed to estimate the precision matrix via adding a sparse-group Lasso-type regularization to the Gaussian negative log-likelihood. Specifically, let  $S$  be an empirical covariance matrix with its  $j$ -th column as  $S_j$ , denote the set of  $p \times p$  square matrices by  $\mathbb{M}^p$  and the set of  $p \times p$  symmetric matrices by  $\mathbb{S}^p$ . The problem of learning a graph with hub nodes can be formulated as the following *hub graphical Lasso* (HGL) optimization problem:

$$\min_{\Theta \in \mathbb{S}^p} \{-\log \det(\Theta) + \langle S, \Theta \rangle + P(\Theta) : \Theta \succ 0\}, \quad (1)$$

where  $\langle S, \Theta \rangle$  is the standard matrix inner product between  $S$  and  $\Theta$ ,  $\Theta \succ 0$  means that  $\Theta \in \mathbb{S}^p$  is positive definite. The function  $P(\Theta)$  is referred to as the *hub penalty*, which takes the form

$$P(\Theta) = \min_{Z \in \mathbb{S}^p, V \in \mathbb{M}^p} \left\{ \lambda_1 \|Z - \text{diag}(Z)\|_1 + \lambda_2 \|V - \text{diag}(V)\|_1 \right. \\ \left. + \lambda_3 \sum_{j=1}^p \|(V - \text{diag}(V))_j\| \mid \Theta = Z + V + V^T \right\}.$$

For any  $x \in \mathbb{R}^p$ , we denote its  $q$ -norm as  $\|x\|_q = (\sum_{i=1}^p |x_i|^q)^{1/q}$ . For simplicity, we denote  $\|\cdot\| = \|\cdot\|_2$ . For any  $X \in \mathbb{M}^p$ , we denote  $\|X\|_1 = \sum_{i=1}^p \sum_{j=1}^p |X_{ij}|$ . This penalty function attempts to decompose the estimated precision matrix  $\Theta$  into three matrices  $Z$ ,  $V$  and  $V^T$ . The non-zero entries of  $Z$  indicate the edges between the non-hub nodes, and the non-zero columns of  $V$  corresponds to the hub nodes. The  $\ell_1$  penalty on the off-diagonal entries of  $Z$  promotes the sparsity of the solution, which reduces the links between the non-hub nodes. The combination of the  $\ell_1$  and  $\ell_2$  penalties for the columns of  $V$  induces group sparsity, which enforces the entries of each column to be either all zeros or almost entirely nonzeros.

However, in the HGL model (1), it is assumed that there are no priors provided for the nodes. That is, there is no *priori* of the hubs. To further make use of the prior knowledge of the hubs that may be available in advance, Bai and Zhou [25] improved the HGL via dividing

the hub penalty in a discriminatory way:

$$\begin{aligned} \tilde{P}(\Theta) = \min_{Z \in \mathbb{S}^p, V \in \mathbb{M}^p} & \left\{ \lambda_1 \|Z - \text{diag}(Z)\|_1 + \lambda_2 \sum_{j \notin \mathcal{D}} \|(V - \text{diag}(V))_j\|_1 \right. \\ & + \lambda_3 \sum_{j \notin \mathcal{D}} \|(V - \text{diag}(V))_j\| + \lambda_4 \sum_{j \in \mathcal{D}} \|(V - \text{diag}(V))_j\|_1 \\ & \left. + \lambda_5 \sum_{j \in \mathcal{D}} \|(V - \text{diag}(V))_j\| \right\} \Big| \Theta = Z + V + V^T, \end{aligned}$$

where  $\mathcal{D} \subseteq \{1, \dots, p\}$  is the index set of hubs with prior information. Here we set  $\lambda_2 \geq \lambda_4$  and  $\lambda_3 \geq \lambda_5$  such that the known hubs are imposed a smaller penalty. It should be noted that the *discriminated hub graphical Lasso* (DHGL) reduces to the HGL if  $\mathcal{D} = \emptyset$ , and reduces to the classical *graphical Lasso* (GL) as  $\lambda_2, \lambda_3, \lambda_4, \lambda_5 \rightarrow \infty$  [43].

Now we directly focus on the DHGL optimization problem. For convenience, we use  $Q(Z)$  and  $R(V)$  to denote the penalty function of  $Z$  and  $V$ , i.e.,

$$Q(Z) = \lambda_1 \|Z - \text{diag}(Z)\|_1, \quad \forall Z \in \mathbb{S}^p,$$

and

$$\begin{aligned} R(V) = & \lambda_2 \sum_{j \notin \mathcal{D}} \|(V - \text{diag}(V))_j\|_1 + \lambda_3 \sum_{j \notin \mathcal{D}} \|(V - \text{diag}(V))_j\| \\ & + \lambda_4 \sum_{j \in \mathcal{D}} \|(V - \text{diag}(V))_j\|_1 + \lambda_5 \sum_{j \in \mathcal{D}} \|(V - \text{diag}(V))_j\|, \quad \forall V \in \mathbb{M}^p. \end{aligned}$$

In addition, we define that  $\log 0 := -\infty$ . Then, the optimization problem can be written as

$$\min_{\Theta, Z \in \mathbb{S}^p, V \in \mathbb{M}^p} \left\{ \langle S, \Theta \rangle - \log \det(\Theta) + Q(Z) + R(V) \Big| \Theta = Z + \mathcal{T}V, \Theta \succeq 0 \right\}, \quad (\text{P})$$

where  $\Theta \succeq 0$  indicates that  $\Theta \in \mathbb{S}^p$  is positive semidefinite, and  $\mathcal{T}: \mathbb{M}^p \rightarrow \mathbb{S}^p$  is a linear operator which is defined as  $\mathcal{T}V := V + V^T$ , for any  $V \in \mathbb{M}^p$ .

To solve the optimization problem HGL or DHGL, Tan et al. [37] applied the *alternating direction method of multipliers* (ADMM) to the problem (1), and Bai and Zhou [25] applied the ADMM to solve the problem (P). (For short, we call this kind of framework as pADMM.) Unfortunately, as the scale of the problems becomes large, the efficiency of the pADMM decreases. On one hand, the ADMM often cannot achieve a solution with high accuracy, which may ruin the performance of the HGL or DHGL model. On the other hand, the computational cost of the ADMM is extremely high and nearly cannot be acceptable when the dimension  $p$  of the data is very high. Hence, an efficient algorithm to solve the problem (P) accurately is needed. For the classical graphical Lasso problem (where  $P(\Theta) = \lambda \|\Theta - \text{diag}\Theta\|_1$ ), a number of optimization algorithms were adopted to solve it, e.g., the ADMM [35], Nesterov's smooth gradient method [9, 26], the block coordinate ascent method [2, 13], the interior point method [43, 24], the Newton method [30, 22], and the dual spectral projected gradient method [29]. Besides, many efficient algorithms have been presented towards other forms of penalty functions. For example, Hsieh et al. [23] employed an iterative quadratic approximation to estimate the precision matrix of the reweighted graphical Lasso model. And the similar idea was also taken

by [41] when considering the fused multiple graphical Lasso problem. In addition, Bybee and Atchadé [5] introduced an approximate majorize-minimize algorithm to compute the Gaussian graphical model with change points. Tarzanagh and Michailidis [38] applied a linearized multi-block ADMM to learn the Gaussian graphical model with structured sparse components. More recently, Zhang et al. [45] proposed a proximal point algorithm to solve the group graphical Lasso problem with the inner subproblem solved by the dual-based semismooth Newton method. Nevertheless, none of these well-designed algorithms can be directly used to solve the DHGL problem. Moreover, in order to solve this kind of large-scale problems, the sparsity structure should be further explored delicately.

In this paper, we develop a two-phase algorithm to compute a high-quality solution of the DHGL problem efficiently. Specifically, in the first phase, we apply the ADMM to the dual of the problem (P) (for short, we call it dADMM), to generate a good initial point to warm start the second phase. In the second phase, we apply the augmented Lagrangian method (ALM) with the subproblems solved by the semismooth Newton (SSN) method to obtain a highly accurate solution. When using the SSN method, we need to thoroughly exploit the sparsity structure of the generalized Jacobian to save the computational cost. The systematic empirical evaluations show that the algorithm is promising and it outperforms the existing pADMM by a large margin in all data settings.

In summary, the contributions of this paper are twofold:

- (1) We design a highly efficient two-phase algorithm to solve the discriminated hub graphical Lasso problem. In particular, we design a surrogate generalized Jacobian of the proximal mapping of the hub penalty, which paves the way for the SSN method to efficiently solve the inner subproblems of the ALM.
- (2) We analyze the convergence of the dADMM, the ALM, and the SSN method. We further conduct systematic experiments to evaluate the proposed algorithm empirically, and the experimental results on both synthetic and real data confirm the general efficacy and the efficiency of our approach.

The rest of this paper is organized as follows. In Section 2, we present the dual of the problem (P) and some necessary preliminaries. In Section 3, we devote to present the two-phase algorithm. In Section 4, we describe the numerical issues for solving the involved subproblems. In Section 5, we implement the numerical experiments to demonstrate the efficacy and efficiency of the proposed algorithm. In Section 6, we conclude this paper.

## 1.1 Additional notations

Let  $\mathcal{X}$ ,  $\mathcal{Y}$  and  $\mathcal{Z}$  be real finite dimensional Euclidean spaces. We denote  $x \circ y$  as the Hadamard product of  $x, y \in \mathcal{X}$ . Let  $f : \mathcal{X} \rightarrow \mathcal{Y}$  and  $g : \mathcal{Y} \rightarrow \mathcal{Z}$ , then  $g \circ f$  denotes the composition of the two functions. Given  $r > 0$ , we denote  $\mathcal{B}_2^r := \{x \in \mathbb{R}^p \mid \|x\| \leq r\}$  and  $\mathcal{B}_\infty^r := \{x \in \mathbb{R}^p \mid \|x\|_\infty \leq r\}$ . For a given closed convex set  $C$  and a vector  $x$ , we denote the Euclidean projection of  $x$  onto  $C$  by  $\Pi_C(x) := \operatorname{argmin}_{y \in C} \|x - y\|$ .

## 2 Preliminaries

In this section, firstly, we formulate the dual problem of the DHGL problem. Then we briefly introduce the proximal mapping and the Moreau envelope, which play important roles in the ALM. Finally, we calculate the proximal mapping and Moreau envelope for the negative log-determinant function  $-\log \det(\cdot)$ , the regularization terms  $Q(\cdot)$  and  $R(\cdot)$  in the DHGL problem.

### 2.1 Duality and the optimality condition

The Lagrangian function associated with the problem (P) is

$$L(\Theta, Z, V; Y) := \langle S, \Theta \rangle - \log \det(\Theta) + Q(Z) + R(V) + \delta_{\mathbb{S}_+^p}(\Theta) - \langle Y, Z + \mathcal{T}V - \Theta \rangle, \quad \forall (\Theta, Z, V, Y) \in \mathbb{S}^p \times \mathbb{S}^p \times \mathbb{M}^p \times \mathbb{S}^p,$$

where  $\delta_{\mathbb{S}_+^p}(\cdot)$  is an indicator function whose effective domain consists of  $p$ -dimensional positive semidefinite matrices. Furthermore, we can obtain the corresponding dual problem:

$$\begin{aligned} \max_{Y, \Omega, \Lambda \in \mathbb{S}^p} \quad & \log \det(\Omega) - Q^*(Y) - R^*(\Lambda) + p \\ \text{s.t.} \quad & S - \Omega + Y = 0, \\ & \Lambda - \mathcal{T}^*Y = 0, \\ & \Omega \succeq 0, \end{aligned} \tag{D}$$

where  $\mathcal{T}^*: \mathbb{S}^p \rightarrow \mathbb{M}^p$  is the adjoint operator of  $\mathcal{T}$ ,  $Q^*(\cdot)$  and  $R^*(\cdot)$  are the Fenchel conjugate functions of  $Q(\cdot)$  and  $R(\cdot)$ , defined by

$$\begin{aligned} Q^*(Y) &= \sup \{ \langle Z, Y \rangle - Q(Z) \mid Z \in \mathbb{S}^p \}, \quad \forall Y \in \mathbb{S}^p, \\ R^*(\Lambda) &= \sup \{ \langle V, \Lambda \rangle - R(V) \mid V \in \mathbb{M}^p \}, \quad \forall \Lambda \in \mathbb{M}^p. \end{aligned}$$

Note that for any  $Y \in \mathbb{S}^p$ , we have  $\mathcal{T}^*Y = 2Y$ . The KKT condition for the problems (P) and (D) is

$$\begin{cases} Z + \mathcal{T}V = \Theta, \\ S - \Omega + Y = 0, \\ \Theta \Omega = I, \\ Y \in \partial Q(Z), \\ \mathcal{T}^*Y \in \partial R(V), \\ \Theta \succeq 0, \quad \Omega \succeq 0. \end{cases} \tag{2}$$

### 2.2 The proximal mapping and the Moreau envelope

In a real finite dimensional Euclidean space  $\mathcal{H}$ , which is equipped with an inner product  $\langle \cdot, \cdot \rangle$  and its induced norm  $\| \cdot \|$ , given a closed convex function  $f: \mathcal{H} \rightarrow \mathbb{R}$ , the Moreau envelope of  $f$  is defined by

$$e_f(x) := \min_{y \in \mathcal{H}} \left\{ f(y) + \frac{1}{2} \|y - x\|^2 \right\}.$$

The unique minimizer of the above minimization problem is called the proximal mapping of  $f$  at  $x$ , and we denote it by  $\text{prox}_f(x)$ . That is,

$$\text{prox}_f(x) := \arg \min_{y \in \mathcal{H}} \left\{ f(y) + \frac{1}{2} \|y - x\|^2 \right\}.$$

It is proven in [34, Theorem 2.26] that the envelope function  $e_f(\cdot)$  is convex and continuously differentiable with

$$\nabla e_f(x) = x - \text{prox}_f(x) = \text{prox}_{f^*}(x),$$

where the last equality is derived by the Moreau identity, which states that the following equation holds for any  $t > 0$  and  $x \in \mathcal{H}$ ,

$$\text{prox}_{tf}(x) + t\text{prox}_{f^*/t}(x/t) = x.$$

### 2.3 Properties of the negative log-determinant function

For convenience, we denote  $h(X) = -\log \det(X)$  for any  $X \succeq 0$ . The proximal mapping of  $h(\cdot)$  and its corresponding Hessian is well studied in [39, Lemma 2.1, Lemma 3.1]. We state them in the following two propositions.

**Proposition 2.1.** *For any  $X \in \mathbb{S}^p$ , let its eigendecomposition be  $X = P \text{Diag}(d) P^T$ , where  $d$  is the vector of eigenvalues in the descending order and  $P$  is an orthonormal matrix whose columns are the corresponding eigenvectors. Given  $\gamma > 0$ , we define two scalar functions*

$$\phi_\gamma^+(x) := \frac{\sqrt{x^2 + 4\gamma} + x}{2} \quad \text{and} \quad \phi_\gamma^-(x) := \frac{\sqrt{x^2 + 4\gamma} - x}{2}, \quad \forall x \in \mathbb{R}.$$

We also define their vector counterparts  $\phi_\gamma^+(\cdot) : \mathbb{R}^p \rightarrow \mathbb{R}^p$  and  $\phi_\gamma^-(\cdot) : \mathbb{R}^p \rightarrow \mathbb{R}^p$  as

$$\phi_\gamma^+(d) := \begin{pmatrix} \phi_\gamma^+(d_1) \\ \vdots \\ \phi_\gamma^+(d_p) \end{pmatrix} \quad \text{and} \quad \phi_\gamma^-(d) := \begin{pmatrix} \phi_\gamma^-(d_1) \\ \vdots \\ \phi_\gamma^-(d_p) \end{pmatrix}, \quad \forall d \in \mathbb{R}^p,$$

and define their matrix counterparts  $\phi_\gamma^+(\cdot) : \mathbb{S}^p \rightarrow \mathbb{S}^p$  and  $\phi_\gamma^-(\cdot) : \mathbb{S}^p \rightarrow \mathbb{S}^p$  as

$$\phi_\gamma^+(X) := P \text{Diag}(\phi_\gamma^+(d)) P^T \quad \text{and} \quad \phi_\gamma^-(X) := P \text{Diag}(\phi_\gamma^-(d)) P^T, \quad \forall X \in \mathbb{S}^p.$$

Now, we have the following two properties:

(i) Both of  $\phi_\gamma^+(X)$  and  $\phi_\gamma^-(X)$  are positive definite for any  $X \in \mathbb{S}^p$ , and

$$X = \phi_\gamma^+(X) - \phi_\gamma^-(X), \quad \langle \phi_\gamma^+(X), \phi_\gamma^-(X) \rangle = \gamma I.$$

(ii) The mapping  $\phi_\gamma^+(\cdot)$  is continuously differentiable and its Fréchet derivative  $(\phi_\gamma^+)'(X)$  is

$$(\phi_\gamma^+)'(X)[H] = P(M \circ (P^T H P)) P^T, \quad \forall H \in \mathbb{S}^p,$$

where  $M \in \mathbb{S}^p$  is defined by

$$M_{ij} = \frac{\phi_\gamma^+(d_i) + \phi_\gamma^+(d_j)}{\sqrt{d_i^2 + 4\gamma} + \sqrt{d_j^2 + 4\gamma}}, \quad i, j = 1, \dots, p.$$

**Proposition 2.2.** *Given  $G \in \mathbb{S}^p$  and  $\sigma > 0$ , we have*

$$\min_{\Omega \succeq 0} \left\{ \frac{1}{2\sigma} \|G - \Omega\|^2 - \log \det(\Omega) \right\} = \frac{1}{2\sigma} \|\phi_\sigma^-(G)\|^2 - \log \det(\phi_\sigma^+(G)),$$

where the minimizer is attained at  $\Omega = \phi_\sigma^+(G)$ . That is,  $\text{prox}_{\sigma h}(G) = \phi_\sigma^+(G)$ .

## 2.4 Properties of the regularization term $Q(\cdot)$

The regularization term  $Q(Z)$  is called the graphical Lasso regularizer [13]:

$$Q(Z) = \lambda_1 \|Z - \text{diag}(Z)\|_1 = \sum_{j=1}^p \lambda_1 \|(Z - \text{diag}(Z))_j\|_1.$$

For  $j = 1, \dots, p$ , let  $Z_{[j]} := [Z_{1j}, \dots, Z_{j-1,j}, 0, Z_{j+1,j}, \dots, Z_{pj}]^T \in \mathbb{R}^p$ , and define  $\mathcal{P}_j : \mathbb{M}^p \rightarrow \mathbb{R}^p$  as a linear map satisfying  $\mathcal{P}_j Z = Z_{[j]}$ . For  $x \in \mathbb{R}^p$ , the adjoint  $\mathcal{P}_j^* : \mathbb{R}^p \rightarrow \mathbb{M}^p$  at  $x$  is defined as  $\mathcal{P}_j^* x$  with placing  $x$  in the  $j$ -th column of a  $p \times p$  all-zero matrix  $X$ , and then setting  $X_{jj}$  to be zero. Additionally, define an operator  $\mathcal{P} : \mathbb{M}^p \rightarrow \mathbb{R}^{p^2}$  as  $\mathcal{P} := [\mathcal{P}_1; \mathcal{P}_2; \dots; \mathcal{P}_p]$ , such that  $\mathcal{P}X$  conducts the operation  $\mathcal{P}_j$  on the  $j$ -th column of  $X$  for all  $j = 1, \dots, p$ , which actually sets the diagonal elements of  $X$  to be zeros and then stacks each column of the corresponding matrix to be a column vector. Thus  $Q(Z) = \sum_{j=1}^p \lambda_1 \|\mathcal{P}_j Z\|_1$ . Then we can compute the closed-form expression of the proximal mapping  $\text{prox}_Q(\cdot)$ , which is stated in the following proposition. We ignore its proof since it is very similar to that of Proposition 2.4.

**Proposition 2.3.** *For any  $Y \in \mathbb{S}^p$ , the proximal operator of  $Q(\cdot)$  at  $Y$  can be computed as*

$$\text{prox}_Q(Y) = \arg \min_{Z \in \mathbb{S}^p} \left\{ \frac{1}{2} \|Z - Y\|^2 + Q(Z) \right\} = Y - \mathcal{P}^* \Pi_{\mathcal{B}_\infty^{p, \lambda_1}}(\mathcal{P}Y),$$

where  $\mathcal{B}_\infty^{p, \lambda_1} := \underbrace{\mathcal{B}_\infty^{\lambda_1} \times \dots \times \mathcal{B}_\infty^{\lambda_1}}_p$ , and  $\Pi_{\mathcal{B}_\infty^{p, \lambda_1}}(\cdot) : \mathbb{R}^{p^2} \rightarrow \mathbb{R}^{p^2}$  is a block-wise projection onto the  $\ell_\infty$

norm ball with the radius  $\lambda_1$ . Specifically, the  $j$ -th block of  $\Pi_{\mathcal{B}_\infty^{p, \lambda_1}}(\mathcal{P}Y)$  is

$$[\Pi_{\mathcal{B}_\infty^{p, \lambda_1}}(\mathcal{P}Y)]_{(j-1)p+1:j p} = \Pi_{\mathcal{B}_\infty^{\lambda_1}}(\mathcal{P}_j Y) = \text{sign}(\mathcal{P}_j Y) \circ \min(|\mathcal{P}_j Y|, \lambda_1), \quad j = 1, \dots, p.$$

Next, for any  $Y \in \mathbb{S}^p$ , we define an alternative for the Clarke generalized Jacobian of  $\text{prox}_Q(\cdot)$  at  $Y$ , i.e.,  $\partial \text{prox}_Q(Y)$ , as below

$$\widehat{\partial} \text{prox}_Q(Y) := \{\mathcal{I} - \mathcal{P}^* \Sigma \mathcal{P} \mid \Sigma \in \partial \Pi_{\mathcal{B}_\infty^{p, \lambda_1}}(\mathcal{P}Y)\}, \quad (3)$$

where  $\partial \Pi_{\mathcal{B}_\infty^{p, \lambda_1}}(\mathcal{P}Y)$  is the Clarke generalized Jacobian of  $\Pi_{\mathcal{B}_\infty^{p, \lambda_1}}(\cdot)$  at  $\mathcal{P}Y$ , which takes the form

$$\partial \Pi_{\mathcal{B}_\infty^{p, \lambda_1}}(\mathcal{P}Y) = \{\text{Diag}(\Sigma_1, \dots, \Sigma_p) \mid \Sigma_j \in \partial \Pi_{\mathcal{B}_\infty^{\lambda_1}}(\mathcal{P}_j Y), \quad j = 1, \dots, p\}.$$

Particularly, for any  $y \in \mathbb{R}^p$ , we have

$$\partial \Pi_{\mathcal{B}_\infty^{\lambda_1}}(y) = \left\{ \text{Diag}(u) \mid u \in \mathbb{R}^p, \quad u_i \in \begin{cases} \{1\} & \text{if } |y_i| < \lambda_1 \\ \{t \mid 0 \leq t \leq 1\} & \text{if } |y_i| = \lambda_1 \\ \{0\} & \text{if } |y_i| > \lambda_1 \end{cases}, \quad i = 1, \dots, p \right\}.$$

Note that it has been proven in [19, Example 2.5] that for any  $H \in \mathbb{S}^p$ ,

$$\widehat{\partial} \text{prox}_Q(Y)[H] = \partial \text{prox}_Q(Y)[H].$$

## 2.5 Properties of the regularization term $R(\cdot)$

The regularization term  $R(\cdot)$  is essentially the weighted group graphical Lasso regularizer:

$$\begin{aligned} R(V) &= \lambda_2 \sum_{j \notin \mathcal{D}} \|(V - \text{diag}(V))_j\|_1 + \lambda_3 \sum_{j \notin \mathcal{D}} \|(V - \text{diag}(V))_j\| \\ &\quad + \lambda_4 \sum_{j \in \mathcal{D}} \|(V - \text{diag}(V))_j\|_1 + \lambda_5 \sum_{j \in \mathcal{D}} \|(V - \text{diag}(V))_j\|, \quad \forall V \in \mathbb{M}^p. \end{aligned}$$

For simplicity, for any  $V \in \mathbb{M}^p$ , we denote

$$\psi(V) = \sum_{j=1}^p w_{1,j} \|(V - \text{diag}(V))_j\|_1, \quad \varphi(V) = \sum_{j=1}^p w_{2,j} \|(V - \text{diag}(V))_j\|,$$

where

$$w_{1,j} = \begin{cases} \lambda_2, & \text{if } j \notin \mathcal{D}, \\ \lambda_4, & \text{if } j \in \mathcal{D}. \end{cases} \quad w_{2,j} = \begin{cases} \lambda_3, & \text{if } j \notin \mathcal{D}, \\ \lambda_5, & \text{if } j \in \mathcal{D}. \end{cases}$$

Then, borrowing the linear operators  $\mathcal{P}_j, j = 1, \dots, p$ , we can write

$$R(V) = \psi(V) + \varphi(V) = \sum_{j=1}^p (w_{1,j} \|\mathcal{P}_j V\|_1 + w_{2,j} \|\mathcal{P}_j V\|). \quad (4)$$

The next proposition provides a crucial property. It reveals that the proximal mapping  $\text{prox}_R(\cdot)$  of  $R = \psi + \varphi$  can be decomposed into the composition of the proximal mappings  $\text{prox}_\psi(\cdot)$  and  $\text{prox}_\varphi(\cdot)$ .

**Proposition 2.4.** *For any  $Y \in \mathbb{M}^p$  and  $\sigma > 0$ , the proximal operator of  $R(\cdot)$  at  $Y$  is*

$$\text{prox}_R(Y) = \text{prox}_\varphi \circ \text{prox}_\psi(Y) = X - \mathcal{P}^* \Pi_{\mathcal{B}_2^{w_2}}(\mathcal{P}X),$$

where

$$\begin{aligned} X &= \text{prox}_\psi(Y) = Y - \mathcal{P}^* \Pi_{\mathcal{B}_\infty^{w_1}}(\mathcal{P}Y), \\ \mathcal{B}_2^{w_2} &:= \mathcal{B}_2^{w_{2,1}} \times \dots \times \mathcal{B}_2^{w_{2,p}}, \quad \mathcal{B}_\infty^{w_1} := \mathcal{B}_\infty^{w_{1,1}} \times \dots \times \mathcal{B}_\infty^{w_{1,p}}, \end{aligned}$$

and  $\Pi_{\mathcal{B}_\infty^{w_1}}(\cdot)$  and  $\Pi_{\mathcal{B}_2^{w_2}}(\cdot)$  are block-wise projections onto  $\ell_\infty$  and  $\ell_2$  norm ball, respectively. Specifically, for  $j = 1, \dots, p$ , the  $j$ -th block of  $\Pi_{\mathcal{B}_\infty^{w_1}}(\mathcal{P}Y)$  and  $\Pi_{\mathcal{B}_2^{w_2}}(\mathcal{P}X)$  are

$$[\Pi_{\mathcal{B}_\infty^{w_1}}(\mathcal{P}Y)]_{(j-1)p+1:jp} = \Pi_{\mathcal{B}_\infty^{w_{1,j}}}(\mathcal{P}_j Y) = \text{sign}(\mathcal{P}_j Y) \circ \min(|\mathcal{P}_j Y|, w_{1,j}),$$

and

$$[\Pi_{\mathcal{B}_2^{w_2}}(\mathcal{P}X)]_{(j-1)p+1:jp} = \Pi_{\mathcal{B}_2^{w_{2,j}}}(\mathcal{P}_j X) = \begin{cases} w_{2,j} \frac{\mathcal{P}_j X}{\|\mathcal{P}_j X\|} & \text{if } \|\mathcal{P}_j X\| > w_{2,j}, \\ \mathcal{P}_j X & \text{otherwise,} \end{cases}$$

respectively.

*Proof.* See Appendix A. □

Note that even though the proximal mapping  $\text{prox}_R(\cdot)$  can be obtained by the composition of  $\text{prox}_\psi(\cdot)$  and  $\text{prox}_\varphi(\cdot)$ , the classical chain rule usually cannot work in calculating the generalized Jacobian of  $\text{prox}_R(\cdot)$  since  $\text{prox}_\psi(\cdot)$  and  $\text{prox}_\varphi(\cdot)$  are non-differentiable [7]. Therefore, we define a surrogate generalized Jacobian of  $\text{prox}_R(\cdot)$  as follows.

**Definition 2.1.** For any  $Y \in \mathbb{M}^p$ ,  $\widehat{\partial}\text{prox}_R(Y) : \mathbb{M}^p \rightrightarrows \mathbb{M}^p$  is defined as

$$\widehat{\partial}\text{prox}_R(Y) := \{(\mathcal{I} - \mathcal{P}^* \Delta \mathcal{P})(\mathcal{I} - \mathcal{P}^* \Xi \mathcal{P}) \mid \Delta \in \partial \Pi_{\mathcal{B}_2^{w_2}}(\mathcal{P}X), \Xi \in \partial \Pi_{\mathcal{B}_\infty^{w_1}}(\mathcal{P}Y)\},$$

where  $X = Y - \mathcal{P}^* \Pi_{\mathcal{B}_\infty^{w_1}}(\mathcal{P}Y)$ , and

$$\begin{aligned} \partial \Pi_{\mathcal{B}_\infty^{w_1}}(\mathcal{P}Y) &= \{\text{Diag}(\Xi_1, \dots, \Xi_p) \mid \Xi_j \in \partial \Pi_{\mathcal{B}_\infty^{w_{1,j}}}(\mathcal{P}_j Y), j = 1, \dots, p\}, \\ \partial \Pi_{\mathcal{B}_2^{w_2}}(\mathcal{P}X) &= \{\text{Diag}(\Delta_1, \dots, \Delta_p) \mid \Delta_j \in \partial \Pi_{\mathcal{B}_2^{w_{2,j}}}(\mathcal{P}_j X), j = 1, \dots, p\}. \end{aligned}$$

For any  $y \in \mathbb{R}^p$  and  $j = 1, \dots, p$ , we have

$$\begin{aligned} \partial \Pi_{\mathcal{B}_\infty^{w_{1,j}}}(y) &= \left\{ \text{Diag}(u) \mid u \in \mathbb{R}^p, u_i \in \begin{cases} \{1\} & \text{if } |y_i| < w_{1,j} \\ \{t \mid 0 \leq t \leq 1\} & \text{if } |y_i| = w_{1,j} \\ \{0\} & \text{if } |y_i| > w_{1,j} \end{cases}, j = 1, \dots, p \right\}, \\ \partial \Pi_{\mathcal{B}_2^{w_{2,j}}}(y) &= \begin{cases} \left\{ \frac{w_{2,j}}{\|y\|} \left( I - \frac{yy^T}{\|y\|^2} \right) \right\} & \text{if } \|y\| > w_{2,j} \\ \left\{ I - t \frac{yy^T}{(w_{2,j})^2} \mid 0 \leq t \leq 1 \right\} & \text{if } \|y\| = w_{2,j} \\ \{I\} & \text{if } \|y\| < w_{2,j} \end{cases}. \end{aligned}$$

Similarly, by [19, Example 2.5] we have that for any  $H \in \mathbb{M}^p$ ,  $\widehat{\partial}\text{prox}_R(Y)[H] = \partial\text{prox}_R(Y)[H]$ .

**Proposition 2.5.**  $\text{prox}_Q(\cdot)$  and  $\text{prox}_R(\cdot)$  are strongly semismooth. That is, let  $X, Y \in \mathbb{S}^p$ , we have

$$\text{prox}_Q(Y) - \text{prox}_Q(X) - \mathcal{W}^Q(Y - X) = O(\|Y - X\|^2), \quad \forall \mathcal{W}^Q \in \widehat{\partial}\text{prox}_Q(Y), \quad (2)$$

and for any  $U, V \in \mathbb{M}^p$ , we have

$$\text{prox}_R(V) - \text{prox}_R(U) - \mathcal{W}^R(V - U) = O(\|V - U\|^2), \quad \forall \mathcal{W}^R \in \widehat{\partial}\text{prox}_R(V). \quad (3)$$

*Proof.* Since  $\text{prox}_Q(\cdot)$  is piecewise affine, according to [12, Proposition 7.4.7] we have (2). Similar to [44, Theorem 3.1], we can easily obtain that (3) holds.  $\square$

### 3 A two-phase algorithm

In this section, we propose a two-phase algorithm to solve the DHGL problem. In Phase I, we adopt the dADMM to generate a nice initial point to warm start the Phase II algorithm. It is worth noting that though the dADMM can be used alone to solve the problem, it is not efficient enough to achieve an accurate solution needed in practical applications. In Phase II, we apply the superlinearly convergent ALM to compute a more accurate solution. Furthermore, in order to fully leverage the sparsity structure of the Jacobians, we use the SSN method to solve the subproblems.

### 3.1 Phase I: dADMM

The minimization form of the dual problem (D) is

$$\begin{aligned} \min_{Y, \Omega, \Gamma, \Lambda \in \mathbb{S}^p} \quad & -\log \det(\Omega) + Q^*(\Gamma) + R^*(\Lambda) + \delta_{\mathbb{S}_+^p}(\Omega) - p \\ \text{s.t.} \quad & S - \Omega + Y = 0, \\ & \Gamma - Y = 0, \\ & \Lambda - \mathcal{T}^*Y = 0. \end{aligned}$$

Its corresponding Lagrangian function is given by

$$\begin{aligned} \mathcal{L}(Y, \Omega, \Gamma, \Lambda; \Theta, Z, V) := & -\log \det(\Omega) + Q^*(\Gamma) + R^*(\Lambda) + \delta_{\mathbb{S}_+^p}(\Omega) - p \\ & - \langle \Theta, S - \Omega + Y \rangle - \langle Z, \Gamma - Y \rangle - \langle V, \Lambda - \mathcal{T}^*Y \rangle, \end{aligned} \quad (4)$$

$$\forall \Omega, Y, \Theta, Z, \Gamma, \Lambda \in \mathbb{S}^p, V \in \mathbb{M}^p.$$

For  $\sigma > 0$ , the associated augmented Lagrangian function is

$$\begin{aligned} \mathcal{L}_\sigma(Y, \Omega, \Gamma, \Lambda; \Theta, Z, V) = & \mathcal{L}(Y, \Omega, \Gamma, \Lambda; \Theta, Z, V) + \frac{\sigma}{2} \|S - \Omega + Y\|^2 \\ & + \frac{\sigma}{2} \|\Gamma - Y\|^2 + \frac{\sigma}{2} \|\Lambda - \mathcal{T}^*Y\|^2. \end{aligned} \quad (5)$$

Based on the augmented Lagrangian function (5), we can adopt the dADMM. We summarize the dADMM for solving the problem (D) in Algorithm 1. One may refer to Section 2 for the detailed computations of the related proximal mappings.

---

#### Algorithm 1 dADMM for DHGL

---

**Input:**  $\Omega^0, \Theta^0 \in \mathbb{S}_{++}^p, Z^0, \Gamma^0, \Lambda^0 \in \mathbb{S}^p, V^0 \in \mathbb{M}^p, \sigma > 0, \tau \in (0, (1 + \sqrt{2})/2)$ , (a typical choice is  $\tau = 1.618$ ). Let  $k = 0$ , iterate as follows:

1: Compute

$$Y^{k+1} = \frac{1}{6\sigma} (\Theta^k - Z^k - V^k - V^{kT}) + \frac{1}{6} (\Gamma^k + 2\Lambda^k - (S - \Omega^k)).$$

2: Compute

$$\begin{cases} \Omega^{k+1} = \phi_{1/\sigma}^+(S + Y^{k+1} - \Theta^k/\sigma), \\ \Gamma^{k+1} = \text{prox}_{Q^*/\sigma}(Y^{k+1} + Z^k/\sigma), \\ \Lambda^{k+1} = \text{prox}_{R^*/\sigma}(\mathcal{T}^*Y^{k+1} + V^k/\sigma). \end{cases}$$

3: Compute

$$\begin{cases} \Theta^{k+1} = \Theta^k - \tau\sigma(S - \Omega^{k+1} + Y^{k+1}), \\ Z^{k+1} = Z^k - \tau\sigma(\Gamma^{k+1} - Y^{k+1}), \\ V^{k+1} = V^k - \tau\sigma(\Lambda^{k+1} - \mathcal{T}^*Y^{k+1}). \end{cases}$$

4:  $k \leftarrow k + 1$ , go to Step 1.

---

Now we give the convergence result of the dADMM for solving the DHGL problem. For clarity and brevity, we simply use  $X_P$  and  $X_D$  to denote the primal and dual variables, respectively, i.e.,  $X_P := (\Theta, Z, V) \in \mathbb{S}_+^p \times \mathbb{S}^p \times \mathbb{M}^p$  and  $X_D := (Y, \Omega, \Gamma, \Lambda) \in \mathbb{S}^p \times \mathbb{S}_+^p \times \mathbb{S}^p \times \mathbb{S}^p$ . Based on [17, Theorem 2], we have the following convergence result.

**Theorem 3.1.** *Let  $\tau \in (0, (1 + \sqrt{5})/2)$ . Let  $\{(X_D^k, X_P^k)\}$  be the sequence generated by the  $dADMM$ . Then  $\{X_D^k := (Y^k, \Omega^k, \Gamma^k, \Lambda^k)\}$  converges to an optimal solution of the problem (D), and  $\{X_P^k := (\Theta^k, Z^k, V^k)\}$  converges to an optimal solution of the problem (P).*

### 3.2 Phase II: ALM

For the ALM, we still work on the augmented Lagrangian function. At the  $k$ -th iteration of the ALM for solving the problem (D), the most important task is to solve the following subproblem

$$\min_{Y, \Omega, \Gamma, \Lambda \in \mathbb{S}^p} \left\{ \mathcal{L}_{\sigma_k}(Y, \Omega, \Gamma, \Lambda; \Theta^k, Z^k, V^k) \right\}, \quad (6)$$

where  $\sigma_k$  is a given parameter,  $(\Theta^k, Z^k, V^k)$  are given points. Since  $\Omega, \Gamma, \Lambda$  are independent of each other, we can solve them separately as follows

$$\begin{aligned} \Omega' &= \phi_{1/\sigma_k}^+(S + Y - \frac{1}{\sigma_k} \Theta^k), \\ \Gamma' &= \text{prox}_{Q^*/\sigma_k}(Y + \frac{1}{\sigma_k} Z^k), \\ \Lambda' &= \text{prox}_{R^*/\sigma_k}(\mathcal{T}^* Y + \frac{1}{\sigma_k} V^k). \end{aligned}$$

Then we can substitute them to the problem (6), we actually solve the subproblem

$$\min_{Y \in \mathbb{S}^p} \Phi_k(Y), \quad (7)$$

where

$$\begin{aligned} \Phi_k(Y) &= \min_{\Omega, \Gamma, \Lambda \in \mathbb{S}^p} \left\{ \mathcal{L}_{\sigma_k}(Y, \Omega, \Gamma, \Lambda; \Theta^k, Z^k, V^k) \right\} \\ &= \sigma_k \left[ (e_{h/\sigma_k})(S + Y - \frac{1}{\sigma_k} \Theta^k) + (e_{Q^*/\sigma_k})(Y + \frac{1}{\sigma_k} Z^k) + (e_{R^*/\sigma_k})(\mathcal{T}^* Y + \frac{1}{\sigma_k} V^k) \right] \\ &\quad - \frac{1}{2\sigma_k} \left( \|\Theta^k\|^2 + \|Z^k\|^2 + \|V^k\|^2 \right) - p. \end{aligned}$$

For clarity, we present the framework of the ALM in Algorithm 2.

---

**Algorithm 2** ALM for DHGL

---

**Input:**  $\Theta^0 \in \mathbb{S}_{++}^p, Z^0 \in \mathbb{S}^p, V^0 \in \mathbb{M}^p; \sigma_0 > 0$ . Let  $k = 0$ , iterate as follows:

1: Compute

$$Y^{k+1} \approx \arg \min_{Y \in \mathbb{S}^p} \Phi_k(Y).$$

2: Compute

$$\begin{aligned} \Omega^{k+1} &= \phi_{1/\sigma_k}^+ \left( S + Y^{k+1} - \frac{1}{\sigma_k} \Theta^k \right), \\ \Gamma^{k+1} &= \text{prox}_{Q^*/\sigma_k} \left( Y^{k+1} + \frac{1}{\sigma_k} Z^k \right), \\ \Lambda^{k+1} &= \text{prox}_{R^*/\sigma_k} \left( \mathcal{T}^* Y^{k+1} + \frac{1}{\sigma_k} V^k \right). \end{aligned}$$

3: Compute

$$\begin{aligned} \Theta^{k+1} &= \Theta^k - \sigma_k (S - \Omega^{k+1} + Y^{k+1}), \\ Z^{k+1} &= Z^k - \sigma_k (\Gamma^{k+1} - Y^{k+1}), \\ V^{k+1} &= V^k - \sigma_k (\Lambda^{k+1} - \mathcal{T}^* Y^{k+1}). \end{aligned}$$

4: Update  $\sigma_{k+1} \uparrow \sigma_\infty$  and  $k \leftarrow k + 1$ , go to Step 1.

---

### 3.2.1 An implementable stopping criteria for the ALM subproblems

Since the subproblem (6) often has no analytical solution, the stopping criteria for the subproblem in the algorithm needs to be discussed. For  $X_D := (Y, \Omega, \Gamma, \Lambda) \in \mathbb{S}^p \times \mathbb{S}_+^p \times \mathbb{S}^p \times \mathbb{S}^p$  and  $X_P := (\Theta, Z, V) \in \mathbb{S}_+^p \times \mathbb{S}^p \times \mathbb{M}^p$ , we define functions  $f_k$  and  $g_k$  as follows

$$\begin{aligned} f_k(X_D) &:= \mathcal{L}_{\sigma_k}(X_D; X_P^k) = \sup_{X_P} \left\{ \mathcal{L}(X_D; X_P) - \frac{1}{2\sigma_k} \|X_P - X_P^k\|^2 \right\}, \\ g_k(X_P) &:= \inf_{X_D} \left\{ \mathcal{L}(X_D; X_P) - \frac{1}{2\sigma_k} \|X_P - X_P^k\|^2 \right\} \\ &= \log \det(\Theta) - \langle S, \Theta \rangle - Q(Z) - R(V) \\ &\quad - \frac{1}{2\sigma_k} (\|\Theta - \Theta^k\|^2 + \|Z - Z^k\|^2 + \|V - V^k\|^2) - \delta_{F_P}(\Theta, Z, V), \end{aligned}$$

where  $F_P := \{(\Theta, Z, V) \mid \Theta - Z - \mathcal{T}V = 0\}$ .

To obtain  $X_D^{k+1}$ , the following criteria on the approximate computation of the subproblem (6) were proposed in [33]:

$$f_k(X_D^{k+1}) - \inf f_k(X_D) \leq \varepsilon_k^2 / (2\sigma_k), \quad \varepsilon_k \geq 0, \quad \sum_{k=0}^{\infty} \varepsilon_k < \infty, \quad (\text{A})$$

$$f_k(X_D^{k+1}) - \inf f_k(X_D) \leq \delta_k^2 / (2\sigma_k) \|X_P^{k+1} - X_P^k\|^2, \quad 0 \leq \delta_k \leq 1, \quad \sum_{k=0}^{\infty} \delta_k < \infty, \quad (\text{B})$$

The convergence results when executing the stopping criteria (A) and (B) for (6) can be obtained directly by adopting [33, Theorem 4, 5]. However, the stopping criteria (A) and (B) are usually not in a direct usage due to the unknown value of  $\inf f_k(X_D)$ . To obtain implementable stopping criteria, we need to find an upper bound for  $f_k(X_D^{k+1}) - \inf f_k(X_D)$ . Since

$$\inf f_k(X_D) = \sup g_k(X_P) \geq g_k(X_P^{k+1}),$$

we have

$$f_k(X_D^{k+1}) - \inf f_k(X_D) \leq f_k(X_D^{k+1}) - g_k(X_P^{k+1}).$$

Hence, we terminate the subproblem (6) if  $(X_D^{k+1}, X_P^{k+1})$  satisfies the following conditions: given nonnegative summable sequences  $\{\varepsilon_k\}$  and  $\{\delta_k\}$  such that  $\delta_k < 1$  for all  $k \geq 0$ ,

$$f_k(X_D^{k+1}) - g_k(X_P^{k+1}) \leq \varepsilon_k^2 / (2\sigma_k), \quad \varepsilon_k \geq 0, \quad \sum_{k=0}^{\infty} \varepsilon_k < \infty, \quad (\text{A}')$$

$$f_k(X_D^{k+1}) - g_k(X_P^{k+1}) \leq \delta_k^2 / (2\sigma_k) \|X_P^{k+1} - X_P\|^2, \quad 0 \leq \delta_k \leq 1, \quad \sum_{k=0}^{\infty} \delta_k < \infty. \quad (\text{B}')$$

### 3.2.2 Convergence results of the ALM

The global convergence and asymptotically superlinear convergence of the ALM have been carefully explored by [33], thus we can directly obtain the result without much effort. Firstly, by denoting  $f(X_P)$  as the objective function of (P)

$$f(X_P) = \langle S, \Theta \rangle - \log \det(\Theta) + Q(Z) + R(V) + \delta_{F_P}(\Theta, Z, V),$$

we can define the maximal monotone operator  $\mathcal{T}_f := \partial f$  and its inverse operator

$$\mathcal{T}_f^{-1}(U_P) = \arg \min_{X_P} \left\{ f_k(X_P) - \langle U_P, X_P \rangle \right\}.$$

Now we are ready to present the convergence result of the ALM for solving the dual problem.

**Theorem 3.2.** (i) Let  $\{(X_D^k, X_P^k)\}$  be the sequence generated by the ALM with the stopping criterion (A'). Then  $\{(X_D^k, X_P^k)\}$  is bounded,  $\{X_D^k\}$  converges to an optimal solution of (D), and  $\{X_P^k\}$  converges to an optimal solution of (P).

(ii) Let  $\rho$  be a positive number such that  $\rho > \sum_{k=0}^{\infty} \varepsilon_k$ . Assume that there exists  $\kappa > 0$  such that

$$\text{dist}(X_P, \mathcal{T}_f^{-1}(0)) \leq \kappa \text{dist}(0, \mathcal{T}_f(X_P))$$

for all  $X_P$  satisfying  $\text{dist}(X_P, \mathcal{T}_f^{-1}(0)) \leq \rho$ . Suppose that the initial point  $X_P^0$  satisfies

$$\text{dist}(X_P^0, \mathcal{T}_f^{-1}(0)) \leq \rho - \sum_{k=0}^{\infty} \varepsilon_k.$$

Let  $\{(X_D^k, X_P^k)\}$  be the sequence generated by the ALM with the stopping criteria (A') and (B'). Then for  $k \geq 0$ , it holds that

$$\text{dist}(X_P^{k+1}, \mathcal{T}_f^{-1}(0)) \leq \varrho_k \text{dist}(X_P^k, \mathcal{T}_f^{-1}(0)),$$

where

$$\varrho_k := \left[ (1 + \delta_k) \kappa (\kappa^2 + \sigma_k^2)^{-1/2} + \delta_k \right] / (1 - \delta_k) \rightarrow \varrho_\infty := \kappa (\kappa^2 + \sigma_\infty^2)^{-1/2},$$

( $\varrho_\infty = 0$  if  $\sigma_\infty = \infty$ ).

### 3.2.3 The SSN for solving the ALM subproblem

Solving the subproblem (7) is the most critical part for the efficiency of the algorithm. By ignoring the superscript, the subproblem at each iteration can be formulated as

$$\min_{Y \in \mathbb{S}^p} \left\{ \Phi(Y) := \sigma \left[ (e_{h/\sigma})(S + Y - \frac{1}{\sigma} \bar{\Theta}) + (e_{Q^*/\sigma})(Y + \frac{1}{\sigma} \bar{Z}) + (e_{R^*/\sigma})(2Y + \frac{1}{\sigma} \bar{V}) \right] - \frac{1}{2\sigma} (\|\bar{\Theta}\|^2 + \|\bar{Z}\|^2 + \|\bar{V}\|^2) - p \right\}, \quad (10)$$

where  $\bar{\Theta}, \bar{Z}, \bar{V}$  are fixed.

Note that  $\Phi(\cdot)$  is strictly convex and continuously differentiable, and for any  $Y \in \mathbb{S}^p$ ,

$$\nabla \Phi(Y) = -\phi_\sigma^+(-\sigma(S + Y) + \bar{\Theta}) + \text{prox}_{\sigma Q}(\sigma Y + \bar{Z}) + 2\text{prox}_{\sigma R}(2\sigma Y + \bar{V}).$$

Thus, the unique solution  $\bar{Y}$  of (10) can be obtained by solving the following nonsmooth system of equations

$$\nabla \Phi(Y) = 0.$$

We adopt the SSN method to solve this nonsmooth system. However, it is difficult to characterize the structure of  $\partial(\nabla \Phi)(Y)$  exactly. Therefore, we also define a multifunction  $\mathcal{V}$  as a surrogate of  $\partial(\nabla \Phi)(Y)$ . The multifunction  $\mathcal{V}: \mathbb{S}^p \rightrightarrows \mathbb{S}^p$  is defined as follows

$$\mathcal{V}(Y) := \sigma \left[ (\phi_\sigma^+)'(-\sigma(S + Y) + \bar{\Theta}) + \hat{\partial} \text{prox}_{\sigma Q}(\sigma Y + \bar{Z}) + 4\hat{\partial} \text{prox}_{\sigma R}(2\sigma Y + \bar{V}) \right].$$

The SSN method is presented in Algorithm 3.

Similar to the proof of [40, Proposition 2], we can prove that  $\nabla \Phi$  is strongly semismooth in combination with Proposition 2.1 and Proposition 2.5, based on which we can get the following convergence result of the SSN method.

**Theorem 3.3.** *Let  $\{Y^j\}$  be the sequence generated by Algorithm 3, then  $\{Y^j\}$  converges to the unique optimal solution  $\bar{Y}$  of (10), and the convergence rate is at least superlinear:*

$$\|Y^{j+1} - \bar{Y}\| = \mathcal{O}(\|Y^j - \bar{Y}\|^{1+\beta}), \quad \beta \in (0, 1].$$

## 4 Numerical issues for solving the subproblem (11)

The most important part in implementing Algorithm 3 is how to efficiently solve the subproblem (11). The Newton system we need to solve is

$$\left[ (\phi_\sigma^+)'(-\sigma(S + Y) + \bar{\Theta})[H] + \mathcal{W}^Q(H) + 4\mathcal{W}^R(H) \right] = -\sigma^{-1} \nabla \Phi(Y), \quad (12)$$

---

**Algorithm 3** SSN for the ALM subproblem
 

---

**Input:**  $\eta \in (0, 1)$ ,  $\beta \in (0, 1]$ ,  $\mu \in (0, 1/2)$ , and  $\delta \in (0, 1)$ . Choose  $Y^0 \in \mathbb{S}^p$  and  $j = 0$ .

- 1: Select  $\mathcal{W}^Q \in \widehat{\partial}\text{prox}_{\sigma Q}(\sigma Y^j + \bar{Z})$ ,  $\mathcal{W}^R \in \widehat{\partial}\text{prox}_{\sigma R}(2\sigma Y^j + \bar{V})$ . Let  $W = \sigma[(\phi_\sigma^+)'(-\sigma(S + Y^j) + \bar{\Theta}) + \mathcal{W}^Q + 4\mathcal{W}^R]$ . Solve the following linear system by the Preconditioned Conjugate Gradient (PCG) method

$$W[H] = -\nabla\Phi(Y^j) \quad (11)$$

to find  $H^j \in \mathbb{S}^p$  such that  $\|W[H^j] + \nabla\Phi(Y^j)\| \leq \min(\eta, \|\nabla\Phi(Y^j)\|^{1+\beta})$ .

- 2: Set  $\alpha_j = \delta^{m_j}$ , where  $m_j$  is the smallest nonnegative integer  $m$  for which

$$\Phi(Y^j + \delta^m H^j) \leq \Phi(Y^j) + \mu\delta^m \langle \nabla\Phi(Y^j), H^j \rangle.$$

- 3: Set  $Y^{j+1} = Y^j + \alpha_j H^j$ .

- 4:  $j \leftarrow j + 1$ , go to Step 1.
- 

where  $\mathcal{W}^Q \in \widehat{\partial}\text{prox}_{\sigma Q}(\sigma Y + \bar{Z})$  and  $\mathcal{W}^R \in \widehat{\partial}\text{prox}_{\sigma R}(2\sigma Y + \bar{V})$ . Here, we can choose  $\mathcal{W}^Q$  and  $\mathcal{W}^R$  such that

$$\mathcal{W}^Q(H) = H - U \circ H, \quad \text{where } U_{ij} = \begin{cases} 0, & \text{if } |(\sigma Y + \bar{Z})_{ij}| > \sigma\lambda_1 \text{ or } i = j, \\ 1, & \text{otherwise,} \end{cases}$$

and

$$\mathcal{W}^R(H) = H - \Sigma^\psi \circ H - \mathcal{P}^* \Sigma^\varphi \mathcal{P}(H - \Sigma^\psi \circ H),$$

where

$$\Sigma_{ij}^\psi = \begin{cases} 0, & \text{if } |(2\sigma Y + \bar{V})_{ij}| > \sigma w_{1,j} \text{ or } i = j, \\ 1, & \text{otherwise,} \end{cases}$$

and

$$\Sigma^\varphi = \text{Diag}(\Sigma_1^\varphi, \dots, \Sigma_p^\varphi),$$

for  $j = 1, \dots, p$ ,

$$\Sigma_j^\varphi = \begin{cases} \frac{\sigma w_{2,j}}{\|z_j\|} \left( I - \frac{z_j z_j^T}{\|z_j\|^2} \right), & \text{if } \|z_j\| > \sigma w_{2,j}, \\ I, & \text{if } \|z_j\| \leq \sigma w_{2,j}, \end{cases}$$

where  $z_j = \mathcal{P}_j X$  with  $X = 2\sigma Y + \bar{V} - \mathcal{P}^* \Pi_{\mathcal{B}_\infty^{w_1}}(\mathcal{P}(2\sigma Y + \bar{V}))$ .

We need to apply the PCG method to solve the system (12). To achieve faster convergence, we hope to devise an easy-to-compute preconditioner. Similar to [39], we define an operator  $\mathcal{T}^\phi : \mathbb{S}^p \rightarrow \mathbb{S}^p$  as  $\mathcal{T}^\phi(H) := P(M \circ (P^T H P)) P^T$ . As we know, the standard basis in  $\mathbb{S}^p$  is given by  $\{E_{ij} := \alpha_{ij}(e_i e_i^T + e_j e_j^T) : 1 \leq i \leq j \leq p\}$ , where  $e_i$  is the  $i$ -th unit vector in  $\mathbb{R}^p$  and  $\alpha_{ij} = 1/\sqrt{2}$  if  $i \neq j$  and  $\alpha_{ij} = 1/2$  otherwise. Let  $\mathbf{T}^\phi$ ,  $\mathbf{W}^Q$  and  $\mathbf{W}^R$  denote the matrix

representations of the linear operators  $\mathcal{T}^\phi$ ,  $\mathcal{W}^Q$  and  $\mathcal{W}^R$ , respectively. Then the diagonal element of  $\mathbf{T}^\phi$  with respect to the basis element  $E_{ij}$  is

$$\begin{aligned} \mathbf{T}_{(ij),(ij)}^\phi &= \langle E_{ij}, \mathcal{T}^\phi(E_{ij}) \rangle = \langle P^T E_{ij} P, M \circ (P^T E_{ij} P) \rangle \\ &= \begin{cases} ((P \circ P)M(P \circ P)^T)_{ij} + \langle v^{(ij)}, Mv^{(ij)} \rangle, & \text{if } i \neq j, \\ ((P \circ P)M(P \circ P)^T)_{ij}, & \text{otherwise,} \end{cases} \end{aligned} \quad (12)$$

where  $v^{(ij)} = P_i \circ P_j$  and  $P_i, P_j$  are the  $i$ th and  $j$ th rows of  $P$ , respectively. The diagonal element of  $\mathbf{W}^Q$  with respect to the basis element  $E_{ij}$  is

$$\mathbf{W}_{(ij),(ij)}^Q = \langle E_{ij}, \mathcal{W}^Q(E_{ij}) \rangle = \langle E_{ij}, E_{ij} - U \circ E_{ij} \rangle = 1 - U_{ij}. \quad (13)$$

The diagonal element of  $\mathbf{W}^R$  with respect to the basis element  $E_{ij}$  is

$$\begin{aligned} \mathbf{W}_{(ij),(ij)}^R &= \langle E_{ij}, \mathcal{W}^Q(E_{ij}) \rangle = \langle E_{ij}, E_{ij} - \Sigma^\psi \circ E_{ij} - \mathcal{P}^* \Sigma^\varphi \mathcal{P}(E_{ij} - \Sigma^\psi \circ E_{ij}) \rangle \\ &= 1 - \Sigma_{ij}^\psi - \langle E_{ij}, \mathcal{P}^* \Sigma^\varphi \mathcal{P}(E_{ij} - \Sigma^\psi \circ E_{ij}) \rangle. \end{aligned} \quad (14)$$

In (12), we note that to compute all the diagonal elements of  $\mathbf{T}^\phi$ , the computational cost of the terms  $\{\langle v^{(ij)}, Mv^{(ij)} \rangle\}_{i,j}$  is  $O(p^4)$  flops. Fortunately, the term  $((P \circ P)M(P \circ P)^T)_{ij}$  is a very good approximation of  $\mathbf{T}_{(ij),(ij)}^\phi$ , whose computational cost is only  $O(p^3)$  flops for all  $i, j$ . Similarly, in (14), the computational cost of the terms  $\{\langle E_{ij}, \mathcal{P}^* \Sigma^\varphi \mathcal{P}(E_{ij} - \Sigma^\psi \circ E_{ij}) \rangle\}_{i,j}$  is also  $O(p^4)$  flops, and  $1 - \Sigma_{ij}^\psi$  is a good approximation to  $\mathbf{W}_{(ij),(ij)}^R$ . Hence, we propose a preconditioner  $\mathcal{V}_D : \mathbb{S}^p \rightarrow \mathbb{S}^p$ , such that

$$\mathcal{V}_D(Y)[H] = D \circ H,$$

where  $D \in \mathbb{S}^p$  and  $D_{ij} = ((P \circ P)M(P \circ P)^T)_{ij} + 1 - U_{ij} + 4(1 - \Sigma_{ij}^\psi)$ , for  $1 \leq i, j \leq p$ .

## 5 Numerical experiments

In this section, we demonstrate the performance of our two-phase algorithm. The pADMM and dADMM serve as benchmark algorithms. We evaluate the efficacy and efficiency of our algorithm on both synthetic and real-world data. The algorithms are implemented in MATLAB R2019a. All the numerical experiments in this paper are carried out on a laptop computer based on 64-bit Windows10 system. The computer is configured as: Intel(R)Core(TM) i5 - 6200U CPU @2.30GHz2.40GHz, 4G running memory.

### 5.1 Experimental setup

#### 5.1.1 Stopping criterion

In our experiments, we define the  $R_P$ ,  $R_D$ , and  $R_C$  to quantify the infeasibilities of the primal and dual problems, and the complementarity condition, where

$$\begin{aligned} R_P &:= \frac{\|\Theta - Z - V - V^T\|}{1 + \|\Theta\|}, & R_D &:= \frac{\|S - \Omega + Y\|}{1 + \|S\|}, \\ R_C &:= \max \left\{ \frac{\|\Theta\Omega - I\|}{1 + \|\Theta\| + \|\Omega\|}, \frac{\|Z - \text{prox}_Q(Y + Z)\|}{1 + \|Z\|}, \frac{\|V - \text{prox}_R(V + \mathcal{T}^*Y)\|}{1 + \|V\|} \right\}. \end{aligned}$$

We stop the algorithm when  $R_P$ ,  $R_D$ , and  $R_C$  achieve a sufficient precision:

$$\max\{R_P, R_D, R_C\} < \text{To1} = 10^{-6}.$$

We also use these three precision metrics to determine when to start Phase II of the algorithm. Particularly, we switch to phase II if  $\max\{R_P, R_D, R_C\} < 10^{-4}$ . Moreover, we fix the maximum iteration numbers of the algorithms. Specifically, in our two-phase algorithm, the Phase I or Phase II algorithm is terminated if the number of the iterations reaches 200. In the benchmark algorithms, we confine the maximum number of iterations to 10,000.

### 5.1.2 Performance measures

Given examples  $\mathbf{x}_1, \dots, \mathbf{x}_n \stackrel{\text{i.i.d.}}{\sim} \mathcal{N}(\mathbf{0}, \Sigma)$  with  $p$  features, the goal of the DHGL is to estimate the inverse of the matrix  $\Sigma$ . Let  $\hat{\Theta}$  be the final estimation of the inverse empirical covariance matrix, we directly regard the entry of  $\hat{\Theta}$  whose value is less than a threshold  $\epsilon$  as 0, such that we can analyze its sparsity pattern. In our experiments, the threshold  $\epsilon$  is fixed to be  $10^{-5}$ . We refer to the index set of the estimated hub nodes by  $\hat{\mathcal{H}}_r$ , and the rule of identifying a node as a hub is that it contains more than  $r$  edges, i.e.,  $\hat{\mathcal{H}}_r = \{i \mid \sum_{j=1, j \neq i}^p (1_{\{|\Omega_{ij}| > \epsilon\}}) > r\}$ . In our experiments, we simply set  $r$  to be  $p/5$ .

**(1) On synthetic data.** The true covariance matrix  $\Sigma$  is known. Thus the true hubs in the graph is available, and we denote the index set of the true hub nodes by  $\mathcal{H}$ . Hence, we can use the following four most commonly used measurements to evaluate the efficacy of the algorithms.

(a) Correctly estimated number of edges:

$$\sum_{j < j'} (1_{\{|\Theta_{jj'}| > \epsilon \text{ and } |\Sigma_{jj'}^{-1}| \neq 0\}}).$$

(b) Proportion of correctly estimated hub nodes:

$$\frac{|\hat{\mathcal{H}}_r \cap \mathcal{H}|}{|\hat{\mathcal{H}}_r|}.$$

(c) Proportion of correctly estimated hub edges:

$$\frac{\sum_{j \in \mathcal{H}, j' \neq j} (1_{\{|\Theta_{jj'}| > \epsilon \text{ and } |\Sigma_{jj'}^{-1}| \neq 0\}})}{\sum_{j \in \mathcal{H}, j' \neq j} (1_{\{|\Sigma_{jj'}^{-1}| \neq 0\}})}.$$

(d) The mean squared error:

$$\mathcal{M}_{\text{MSE}} := \frac{\sum_{j < j'} (\Theta_{jj'} - \Sigma_{jj'}^{-1})^2}{p(p-1)}.$$

**(2) On real-world data.** In the case of real data, the actual covariance matrix  $\Sigma$  is unknown and cannot be evaluated using the previous four measurements, so we only compare the computational time for different algorithms.

### 5.1.3 Hyperparameter tuning

Similar to other machine learning models, the hyperparameter tuning also plays a critical role in the DHGL. Tan et al. [37] proposed to select the hyperparameters by optimizing a Bayesian information criterion (BIC)-type quantity, but this quantity tends to yield unnecessarily dense graphs when the dimension  $p$  is large [11], and it also introduces two additional hyperparameters that are too sensitive to the quality of the solution. As a result, instead of using the BIC-type quantity, we adopt the conventional  $k$ -fold cross-validation [4], and set  $k = 5$  in our experiments.

For each hyperparameter, we set different search scopes, respectively. In our experiments, we fix  $\lambda_1 = 0.4$ , and consider the cases where  $\lambda_3 \in \{1, 1.5, 2\}$  and  $\lambda_5 \in \{0.5, 1\}$ . For the tuning of  $\lambda_2$  and  $\lambda_4$ , we use a relatively finer grid of their values. For details, we select  $\lambda_2$  from  $[0.1, 0.5]$  and  $\lambda_4$  from  $[0.05, 0.15]$ .

Another problem in the hyperparameter tuning is to specify the index set  $\mathcal{D}$ , which indicates the possible hubs. Li, Bai, and Zhou [25] recommended employing the GL or HGL before applying the DHGL to identify the hubs previously, and designed two individual strategies towards various cases where the hubs are known or unknown. For completeness, we include their proposed strategies in Algorithms 4 and 5. Furthermore, we note that the proposed strategies also alleviate the difficulty in hyperparameter selections because the setting of the hyperparameters in the HGL can be directly adapted to the DHGL.

---

**Algorithm 4** DHGL with known hubs

---

- 1: Using the HGL with cross-validation to obtain the estimated hubs, denoted by  $\mathcal{H}_{\text{HGL}}$ .
  - 2: Set  $\mathcal{D} = \mathcal{K} \setminus \mathcal{H}_{\text{HGL}}$ , where  $\mathcal{K}$  is the set of known hubs.
  - 3: If  $\mathcal{D} \neq \emptyset$ , get the estimation  $\Theta$  by solving the DHGL, and denote the estimated hubs by  $\mathcal{H}_{\text{DHGL}}$ , where  $\lambda_1, \lambda_2, \lambda_3$  are directly set by the same values as those in the HGL and  $\lambda_4, \lambda_5$  are selected based on the cross-validation. Then let  $\mathcal{H}_r = \mathcal{H}_{\text{HGL}} \cup \mathcal{H}_{\text{DHGL}}$  as the set of the estimated hubs. If  $\mathcal{D} = \emptyset$ , use the estimation  $\Theta$  of the HGL as the final estimation result, and let  $\mathcal{H}_r = \mathcal{H}_{\text{HGL}}$ .
- 

---

**Algorithm 5** DHGL with unknown hubs

---

- 1: Using the HGL with cross-validation to obtain the estimated hubs, denoted by  $\mathcal{H}_{\text{HGL}}$ .
  - 2: (Prior Information Construction) Tune the regularization parameter  $\lambda$  of the GL from large to small until  $|\mathcal{H}_{\text{GL}} \setminus \mathcal{H}_{\text{HGL}}| > 0$  and  $|\mathcal{H}_{\text{GL}} \cup \mathcal{H}_{\text{HGL}}| \leq \max\{|\mathcal{H}_{\text{HGL}} + a, b|\mathcal{H}_{\text{HGL}}|\}$ , where  $a, b$  are typically set to be 2 and 1.1.
  - 3: Set  $\mathcal{D} = \mathcal{H}_{\text{GL}} \setminus \mathcal{H}_{\text{HGL}}$  which is nonempty.
  - 4: Use the DHGL to estimate  $\Theta$ , where  $\lambda_1, \lambda_2, \lambda_3$  remain the same values as those in the HGL,  $\lambda_4$  is equally set to be  $\lambda_2$ , and  $\lambda_5$  is selected using the cross-validation.
- 

## 5.2 Experiments on synthetic data

We consider two cases (the hubs are known or unknown) and apply the corresponding strategies. We apply three different algorithms to solve the core optimization problems (i.e., HGL and DHGL).

Now, we introduce three simulation settings used for the evaluation. We first randomly generate a  $p \times p$  adjacency matrix on the basis of the following three set-ups.

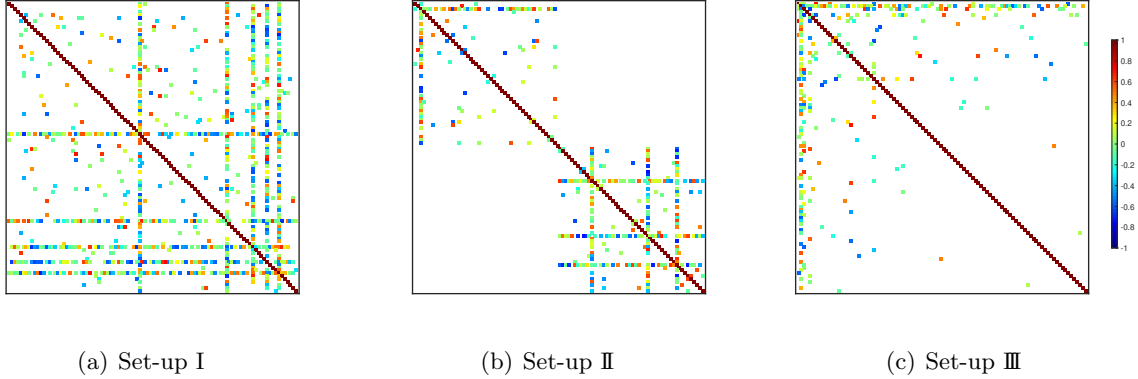


**Figure 1:** Examples of the inverse covariance matrix in three set-ups.

I - Network with hub nodes. We randomly select  $|\mathcal{H}|$  nodes as the hubs. For any  $i < j$ , we set the probability of  $A_{ij} = 1$  to be 0.7 if the corresponding node is the hub and to be 0.02 otherwise. That is, for any  $i < j$ , we have

$$\text{Prob}(A_{ij} = 1) = \begin{cases} 0.7, & \text{if } i \in \mathcal{H}, \\ 0.02, & \text{otherwise.} \end{cases}$$

Finally, the adjacency matrix  $A$  is completed by setting  $A_{ji} = A_{ij}$  for  $i = 1, \dots, p$ .

II - Network consisting of two connected subnetworks with hub nodes. The adjacency matrix  $A = \begin{pmatrix} A_1 & 0 \\ 0 & A_2 \end{pmatrix}$ , where  $A_1$  and  $A_2$  are generated in accordance with the set-up I.

III - Scale-free network. For any given node, the probability that it has  $k$  edges is proportional to  $k^{-\alpha}$ . For this simulation setting, we use the graph library NetworkX [16] to generate the adjacency matrix.

Next, we use the adjacency matrix  $A$  to create a matrix  $E$ . To be specific, for any  $(i, j)$  such that  $A_{ij} \neq 0$ , let  $E_{ij}$  follow a uniform distribution with the interval  $[-0.75, -0.25] \cup [0.25, 0.75]$ , i.e., in other words,

$$E_{ij} \stackrel{\text{i.i.d.}}{\sim} \begin{cases} 0, & \text{if } A_{ij} = 0, \\ \text{Unif}([-0.75, -0.25] \cup [0.25, 0.75]), & \text{otherwise.} \end{cases}$$

Then, we can obtain a symmetric matrix  $\bar{E}$  by setting  $\bar{E} = (E + E^T)/2$ . The inverse covariance matrix is constructed by setting  $\Sigma^{-1} = \bar{E} + (0.1 - \rho_{\min}(\bar{E}))I$ , where  $\rho_{\min}(\bar{E})$  indicates the smallest eigenvalue of  $\bar{E}$ . Now, we can generate the data matrix  $X = (\mathbf{x}_1; \dots; \mathbf{x}_n)$ , where each row is sampled from the normal distribution  $\mathcal{N}(0, \Sigma)$ . Finally, we conduct an additional standardization, such that the standard deviation of each feature is equal to one. To clearly illustrate the generated inverse covariance matrix  $\Sigma^{-1}$ , we also give an example in Figure 1 for each set-up.

For the generated data matrix  $X \in \mathbb{R}^{n \times p}$ , we considered the following seven cases:

$$(n, p) \in \{(100, 300), (300, 500), (500, 800), (800, 1000), (1000, 1500), (1500, 2000), (2000, 2500)\}.$$

We also need to set the number of the true hub nodes (i.e., the cardinality of the hub index set  $|\mathcal{H}|$ ) in set-up I and II. In our experiments, we set  $|\mathcal{H}|$  to be 5, 5, 10, 10, 30, 30 and 30, respectively for each case. Besides, the cardinality  $|\mathcal{H}|$  in set-up III is dependent on the generated adjacency matrix rather than our setting. In this simulation setting, a node will be identified as a hub if it has more than  $r$  edges, i.e.,  $\mathcal{H} = \{i \mid \sum_{j=1, j \neq i}^p A_{ij} > r, i = 1, \dots, p\}$ , and we also set  $r = p/5$ .

### 5.2.1 Experiments with known hub nodes

When the hub nodes are known, for the DHGL problem, the numerical performances of the pADMM, dADMM and two-phase algorithms on the synthetic data of simulation settings I, II and III are compared. The specific numerical performances are listed in the tables below, where “P”, “D”, “T”, “T(I)” and “T(II)” denote the pADMM, dADMM, two-phase algorithm, Phase I algorithm and Phase II algorithm, respectively, and the computational time is recorded in the format of “hours:minutes:seconds”. As can be seen from the numerical test results in Tables 1-3, for the synthetic data of known hubs, the two-phase algorithm is more efficient than the pADMM and dADMM in all the cases.

Table 1 In simulation setting I, the test results for the DHGL problem in which the hub nodes are known

$(n, p)$	$\max\{R_P, R_D, R_C\}$			iter				time		
	P	D	T	P	D	T(I)	T(II)	P	D	T
(100, 300)	9.84e-07	9.90e-07	1.29e-07	471	594	200	12(19)	0:00:11	00:00:18	00:00:10
(300, 500)	9.34e-07	9.89e-07	1.14e-07	518	329	126	7(8)	00:00:53	00:00:39	00:00:19
(500, 800)	9.33e-07	9.93e-07	1.91e-07	781	339	135	5(6)	00:04:13	00:02:25	00:01:09
(800, 1000)	9.81e-07	9.70e-07	9.80e-07	955	366	126	4(5)	00:08:42	00:06:02	00:01:35
(1000, 1500)	9.90e-07	9.94e-07	8.87e-07	1378	900	200	37(45)	00:33:21	00:27:34	00:19:28
(1500, 2000)	1.00e-06	9.83e-07	5.01e-07	1609	646	200	12(13)	01:19:47	00:39:53	00:18:16
(2000, 2500)	9.99e-07	9.96e-07	5.12e-07	2857	1693	200	31(44)	04:07:22	03:09:18	01:06:12

Table 2 In simulation setting II, the test results for the DHGL problem in which the hub nodes are known

$(n, p)$	$\max\{R_P, R_D, R_C\}$			iter				time		
	P	D	T	P	D	T(I)	T(II)	P	D	T
(100, 300)	9.99e-07	9.89e-07	5.62e-07	490	317	200	12(16)	00:00:12	00:00:10	00:00:07
(300, 500)	9.96e-07	9.84e-07	8.21e-07	683	372	200	12(14)	00:01:15	00:00:44	00:00:31
(500, 800)	9.99e-07	9.89e-07	3.85e-07	781	484	200	13(22)	00:04:16	00:03:11	00:02:15
(800, 1000)	9.96e-07	9.84e-07	7.19e-07	1056	551	200	13(20)	00:09:30	00:06:11	00:03:41
(1000, 1500)	9.95e-07	9.91e-07	4.71e-07	1293	908	200	15(23)	00:31:02	00:27:12	00:11:21
(1500, 2000)	9.98e-07	9.96e-07	7.95e-07	2012	1112	200	15(16)	01:50:30	01:09:27	00:17:12
(2000, 2500)	9.98e-07	9.99e-07	5.13e-07	1764	1367	200	18(34)	02:55:01	02:36:06	01:04:21

Table 3 In simulation setting III, the test results for the DHGL problem in which the hub nodes are known

$(n, p)$	$\max\{R_P, R_D, R_C\}$			iter				time		
	P	D	T	P	D	T(I)	T(II)	P	D	T
(100, 300)	9.89e-07	9.77e-07	3.59e-07	449	338	200	13(16)	00:00:10	00:00:11	00:00:09
(300, 500)	9.99e-07	9.82e-07	2.67e-07	714	359	200	12(13)	00:01:15	00:00:49	00:00:35
(500, 800)	9.93e-07	9.90e-07	5.01e-07	688	505	200	12(12)	00:03:43	00:03:54	00:01:52
(800, 1000)	9.96e-07	9.84e-07	3.60e-07	1058	546	200	13(13)	00:09:52	00:09:19	00:03:13
(1000, 1500)	9.93e-07	9.97e-07	3.13e-07	778	606	200	14(20)	00:20:18	00:21:09	00:09:50
(1500, 2000)	9.98e-07	9.96e-07	4.09e-07	1401	968	200	14(14)	01:15:24	01:22:27	00:21:02
(2000, 2500)	9.95e-07	9.94e-07	5.07e-07	2609	1402	200	17(21)	04:30:37	03:48:58	01:11:18

### 5.2.2 Results with unknown hub nodes

When the hub nodes are unknown, for the DHGL problem, the numerical performances of the pADMM, dADMM and two-phase algorithms on the synthetic data of simulation Settings I, II and III are compared. The specific numerical performances are shown in the tables below. As can be seen from the numerical test results in Tables 4-6, for the synthetic data of unknown hubs, the two-phase algorithm is the most efficient algorithm in all the cases.

Table 4 In simulation setting I, the test results for the DHGL problem of the hub node are unknown

$(n, p)$	$\max\{R_P, R_D, R_C\}$			iter				time		
	P	D	T	P	D	T(I)	T(II)	P	D	T
(100, 300)	9.92e-07	9.98e-07	2.34e-07	737	483	200	12(21)	00:00:19	00:00:15	00:00:11
(300, 500)	9.93e-07	9.92e-07	5.44e-07	1038	636	200	12(12)	00:01:50	00:01:22	00:00:31
(500, 800)	9.98e-07	9.92e-07	3.94e-07	1443	954	200	14(14)	00:07:55	00:06:55	00:01:50
(800, 1000)	9.96e-07	8.96e-07	7.50e-07	1610	976	200	14(14)	00:15:02	00:12:10	00:04:17
(1000, 1500)	1.00e-06	9.95e-07	2.52e-07	2238	1579	200	19(24)	00:55:42	00:51:59	00:12:12
(1500, 2000)	9.98e-07	9.95e-07	4.43e-07	2784	2003	200	17(17)	02:27:29	02:51:18	00:21:21
(2000, 2500)	9.99e-07	1.00e-06	4.96e-07	3954	2505	200	19(53)	06:31:37	05:45:03	02:23:26

Table 5 In simulation setting II, the test results for the DHGL problem of the hub node are unknown

$(n, p)$	$\max\{R_P, R_D, R_C\}$			iter				time		
	P	D	T	P	D	T(I)	T(II)	P	D	T
(100, 300)	9.87e-07	9.93e-07	4.54e-07	658	418	200	11(11)	00:00:16	00:00:12	00:00:08
(300, 500)	9.95e-07	9.84e-07	4.40e-07	861	372	200	12(19)	00:01:29	00:00:45	00:00:36
(500, 800)	9.92e-07	9.89e-07	2.06e-07	929	484	200	13(13)	00:04:57	00:03:21	00:01:38
(800, 1000)	9.97e-07	9.84e-07	3.79e-07	1043	551	200	13(13)	00:12:52	00:09:35	00:02:48
(1000, 1500)	9.94e-07	9.91e-07	2.51e-07	1531	908	200	15(15)	00:39:33	00:32:09	00:07:34
(1500, 2000)	9.96e-07	9.96e-07	4.25e-07	1860	1112	200	15(15)	01:43:56	01:15:23	00:15:25
(2000, 2500)	9.98e-07	9.99e-07	2.77e-07	2446	1367	200	18(18)	04:01:29	02:59:30	00:34:40

Table 6 In simulation setting III, the test results for the DHGL problem of the hub node are unknown

$(n, p)$	$\max\{R_P, R_D, R_C\}$			iter				time		
	P	D	T	P	D	T(I)	T(II)	P	D	T
(100, 300)	9.90e-07	9.99e-07	5.18e-07	438	259	200	10(10)	00:00:10	00:00:09	00:00:08
(300, 500)	9.92e-07	9.95e-07	4.67e-07	591	380	200	10(16)	00:01:01	00:00:53	00:00:42
(500, 800)	9.92e-07	9.83e-07	2.34e-07	1051	485	200	12(12)	00:05:39	00:04:18	00:01:53
(800, 1000)	9.96e-07	9.94e-07	3.42e-07	959	557	200	12(12)	00:08:53	00:06:57	00:03:29
(1000, 1500)	9.97e-07	9.96e-07	3.18e-07	1341	937	200	14(14)	00:35:25	00:39:04	00:09:12
(1500, 2000)	9.98e-07	9.92e-07	4.34e-07	1470	853	200	15(15)	01:22:28	01:14:32	00:22:33
(2000, 2500)	9.98e-07	9.89e-07	2.80e-07	2596	793	200	16(16)	04:06:21	01:30:01	00:29:11

In order to explain the graph recovery of the three algorithms more intuitively, we select an example with dimension  $p = 800$  for the simulation setting II , and draw the estimated adjacency matrix.

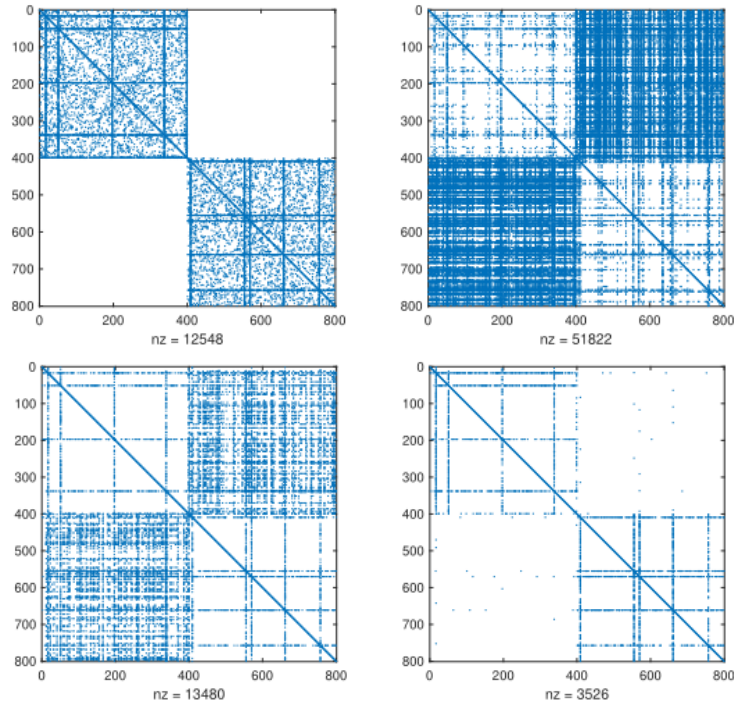


**Figure 2:** The adjacency matrix of graph estimation by using three algorithms. The four subfigures are the true adjacency matrix (i.e., ground truth), the estimation results of the pADMM, dADMM, and two-phase algorithm, respectively. The number of the non-zero elements is denoted by  $nz$ .

It can be seen from Figure 2 that the estimations via the pADMM and dADMM contain a large number of wrong edges. However, the two-phase algorithm still converges well and accurately identifies all the hub nodes.

Meanwhile, in order to illustrate the efficacy of the two-phase algorithm, we draw the relevant data of four criteria (the same as those in [37]) to evaluate the efficacy of the algorithm in seven different dimensions for the simulation setting I when the hub nodes are known. As can be seen from Figure 3, the two-phase algorithm performs well in the correct estimation of the number of edges, the proportion of correctly estimated hub nodes, the proportion of correctly estimated hub edges, and the mean squared error, which also fully demonstrate the efficacy of the two-phase algorithm.

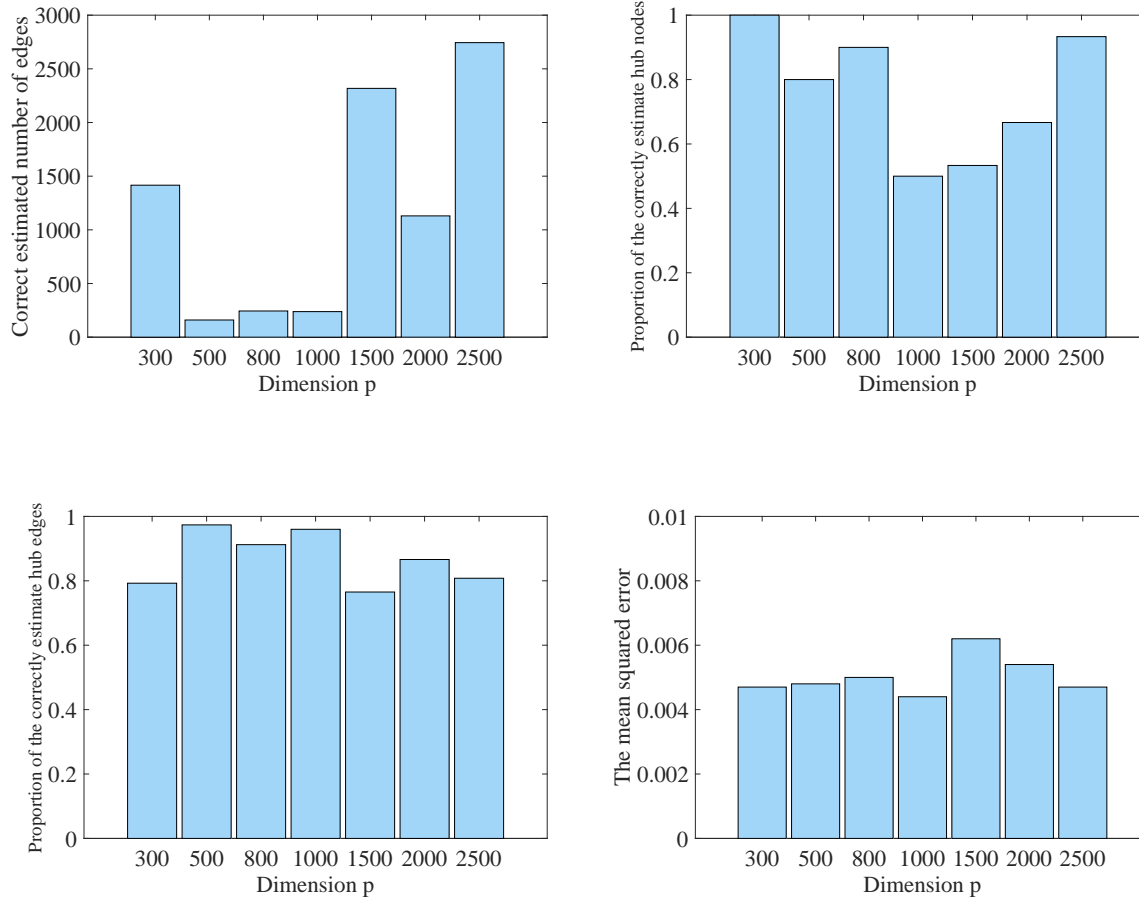


**Figure 3:** Results of synthetic data efficacy measures

### 5.3 Experiments on real-world data

For the DHGL problem, the numerical performances of the pADMM, dADMM and two-phase algorithm on the following five real data are compared. We list the numerical performance in the table below. As can be seen from the numerical test results in Table 7, the two-phase algorithm can obtain the desired solutions with the given accuracy for all data sets. In contrast, for most cases, the pADMM and dADMM reach the maximal number of iterations and cannot obtain the corresponding results with the given accuracy. Meanwhile, the computational time of the

two-phase algorithm is much less than that of the pADMM and dADMM.

Table 7 For real data, the test results of the DHGL problem

name( $n, p$ )	$\max\{R_P, R_D, R_C\}$			iter				time		
	P	D	T	P	D	T(I)	T(II)	P	D	T
Iconix(10455, 255)	3.27e-03	1.56e-02	5.78e-07	10000	10000	200	28(44)	00:04:00	00:03:31	00:00:10
Rosetta(6316, 301)	6.35e-03	2.88e-02	6.67e-07	10000	10000	200	29(35)	00:04:22	00:05:05	00:00:13
animals(33, 102)	5.12e-05	9.99e-07	9.43e-07	10000	6545	200	14(14)	00:00:42	00:00:33	00:00:02
cancer(20531, 801)	6.11e-03	9.74e-02	9.23e-07	10000	10000	200	25(45)	00:59:37	01:07:35	00:02:41
zoo(100, 17)	9.97e-07	1.00e-06	5.39e-07	2935	1347	200	14(14)	00:00:03	00:00:02	00:00:01

## 6 Conclusion

In this paper, we have developed a two-phase algorithm to solve the hub graphical Lasso model with the structured sparsity. Specifically, we design the dADMM in Phase I to generate a good initial point to warm start Phase II of the ALM. The SSN method is applied to solve the inner subproblems of the ALM. We take full advantage of the sparsity structure of the generalized Jacobian and make the performances of the SSN and ALM efficiently. Numerical experiments on both synthetic data and real data have demonstrated the efficacy and efficiency of the proposed algorithm.

## A Proof of Proposition 2.4

*Proof.* Firstly, we calculate the proximal operators of  $\varphi$  and  $\psi$ . Since for any  $V \in \mathbb{M}^p$ ,

$$\varphi(V) = \sum_{j=1}^p w_{2,j} \|\mathcal{P}_j V\|,$$

by denoting  $\widehat{\mathcal{P}}_j : \mathbb{R}^p \rightarrow \mathbb{R}^p$  as  $\widehat{\mathcal{P}}_j y = [y_1; \dots; y_{j-1}; 0; y_{j+1}; \dots; y_p]$  for any  $y \in \mathbb{R}^p$ , we have that

$$\begin{aligned} \varphi^*(Y) &= \sup_{V \in \mathbb{M}^p} \left\{ \langle Y, V \rangle - \sum_{j=1}^p w_{2,j} \|\mathcal{P}_j V\| \right\} \\ &= \sum_{j=1}^p \sup_{V_j \in \mathbb{R}^p} \left\{ \langle Y_j, V_j \rangle - w_{2,j} \|\widehat{\mathcal{P}}_j V_j\| \right\} \\ &= \sum_{j=1}^p \sup_{V_j \in \mathbb{R}^p} \left\{ Y_{jj} V_{jj} + \langle \mathcal{P}_j Y, \widehat{\mathcal{P}}_j V_j \rangle - w_{2,j} \|\widehat{\mathcal{P}}_j V_j\| \right\}. \end{aligned}$$

Note that

$$Y_{jj} V_{jj} + \langle \mathcal{P}_j Y, \widehat{\mathcal{P}}_j V_j \rangle - w_{2,j} \|\widehat{\mathcal{P}}_j V_j\| \leq Y_{jj} V_{jj} + \|\widehat{\mathcal{P}}_j V_j\| (\|\mathcal{P}_j Y\| - w_{2,j}).$$

Therefore,

$$\varphi^*(Y) = \delta_C(Y),$$

where  $C := \{Y \in \mathbb{M}^p \mid \|\mathcal{P}_j Y\| \leq w_{2,j} \text{ and } Y_{jj} = 0, j = 1, 2, \dots, p\}$ . Then by the Moreau identity, we have

$$\text{prox}_\varphi(Y) = Y - \text{prox}_{\varphi^*}(Y) = Y - \Pi_C(Y) = Y - \mathcal{P}^* \Pi_{\mathcal{B}_2^{w_2}}(\mathcal{P}Y),$$

where

$$[\Pi_{\mathcal{B}_2^{w_2}}(\mathcal{P}Y)]_{(j-1)p+1:jp} = \Pi_{\mathcal{B}_2^{w_{2,j}}}(\mathcal{P}_j Y) = \begin{cases} w_{2,j} \frac{\mathcal{P}_j Y}{\|\mathcal{P}_j Y\|} & \text{if } \|\mathcal{P}_j Y\| > w_{2,j}, \\ \mathcal{P}_j Y & \text{otherwise.} \end{cases} \quad (15)$$

Similarly, we can calculate that

$$\text{prox}_\psi(Y) = Y - \mathcal{P}^* \Pi_{\mathcal{B}_\infty^{w_1}}(\mathcal{P}Y),$$

where

$$[\Pi_{\mathcal{B}_\infty^{w_1}}(\mathcal{P}Y)]_{(j-1)p+1:jp} = \Pi_{\mathcal{B}_\infty^{w_{1,j}}}(\mathcal{P}_j Y) = \text{sign}(\mathcal{P}_j Y) \circ \min(|\mathcal{P}_j Y|, w_{1,j}).$$

In the following, we prove the result about the proximal mapping of  $R(\cdot)$ . We can see from (4) that the function  $R(V)$  has a separable structure, thus we only need to prove that

$$\text{prox}_{w_{1,j}\|\mathcal{P}_j \cdot\|_1 + w_{2,j}\|\mathcal{P}_j \cdot\|}(Y) = \text{prox}_{w_{2,j}\|\mathcal{P}_j \cdot\|} \circ \text{prox}_{w_{1,j}\|\mathcal{P}_j \cdot\|_1}(Y), \quad j = 1, 2, \dots, p.$$

By [42, Theorem 1], it suffices to show that for each  $j = 1, \dots, p$ ,

$$\partial(w_{1,j}\|\mathcal{P}_j Y\|_1) \subseteq \partial(w_{1,j}\|\mathcal{P}_j Z\|_1),$$

where  $Z = \text{prox}_\varphi(Y) = Y - \mathcal{P}^* \Pi_{\mathcal{B}_2^{w_2}}(\mathcal{P}Y)$ . We prove this relation in two cases:

(1) If  $\|\mathcal{P}_j Y\| \leq w_{2,j}$ , from (15), we have  $\mathcal{P}_j Z = 0$ . Then according to [32, Theorem 23.9], we obtain

$$\partial(w_{1,j}\|\mathcal{P}_j Z\|_1) = \left\{ \mathcal{P}_j^* v \mid v \in [-w_{1,j}, w_{1,j}]^p \right\},$$

which contains  $\partial(w_{1,j}\|\mathcal{P}_j Y\|_1)$ .

(2) If  $\|\mathcal{P}_j Y\| > w_{2,j}$ , from (15), we have  $\mathcal{P}_j Z = (1 - \frac{w_{2,j}}{\|\mathcal{P}_j Y\|})(\mathcal{P}_j Y)$ , which implies  $\text{sign}(\mathcal{P}_j Y) = \text{sign}(\mathcal{P}_j Z)$ . Therefore,  $\partial(w_{1,j}\|\mathcal{P}_j Y\|_1) \subseteq \partial(w_{1,j}\|\mathcal{P}_j Z\|_1)$ .

Now we have finished all the proof.  $\square$

## References

- [1] R. ALBERT, *Scale-free networks in cell biology*, Journal of Cell Science, 118 (2005), pp. 4947–4957.
- [2] O. BANERJEE, L. EL GHAOU, AND A. D’ASPREMONT, *Model selection through sparse maximum likelihood estimation for multivariate Gaussian or binary data*, Journal of Machine Learning Research, 9 (2008), pp. 485–516.
- [3] A.-L. BARABASI AND Z. N. OLTVAI, *Network biology: Understanding the cell’s functional organization*, Nature Reviews Genetics, 5 (2004), pp. 101–113.

- [4] P. J. BICKEL AND E. LEVINA, *Regularized estimation of large covariance matrices*, The Annals of Statistics, 36 (2008), pp. 199–227.
- [5] L. BYBEE AND Y. ATCHADÉ, *Change-point computation for large graphical models: A scalable algorithm for Gaussian graphical models with change-points*, Journal of Machine Learning Research, 19 (2018), pp. 1–38.
- [6] A. CHATURVEDI AND J. SCARLETT, *Learning Gaussian graphical models via multiplicative weights*, in International Conference on Artificial Intelligence and Statistics, PMLR, 2020, pp. 1104–1114.
- [7] F. CLARKE, *Optimization and Nonsmooth Analysis*, John Wiley and Sons, New York, 1983.
- [8] D. COX AND N. WERMUTH, *Multivariate Dependencies: Models, Analysis and Interpretation*, Chapman & Hall/CRC Monographs on Statistics & Applied Probability, CRC Press, 2014.
- [9] A. D’ASPREMONT, O. BANERJEE, AND L. EL GHAOUI, *First-order methods for sparse covariance selection*, SIAM Journal on Matrix Analysis and Applications, 30 (2008), pp. 56–66.
- [10] A. DEFAZIO AND T. CAETANO, *A convex formulation for learning scale-free networks via submodular relaxation*, in Advances in Neural Information Processing Systems, vol. 25, Curran Associates, Inc., 2012.
- [11] M. DRTON AND M. H. MAATHUIS, *Structure learning in graphical modeling*, Annual Review of Statistics and Its Application, 4 (2017), pp. 365–393.
- [12] F. FACCHINEI AND J.-S. PANG, *Finite-Dimensional Variational Inequalities and Complementarity Problems*, vol. II, Springer, 2003.
- [13] J. FRIEDMAN, T. HASTIE, AND R. TIBSHIRANI, *Sparse inverse covariance estimation with the graphical lasso*, Biostatistics, 9 (2008), pp. 432–441.
- [14] X. GAO, W. SHEN, C.-M. TING, S. C. CRAMER, R. SRINIVASAN, AND H. OMBAO, *Modeling brain connectivity with graphical models on frequency domain*, arXiv preprint arXiv:1810.03279, (2018).
- [15] N. HAFIENE, W. KAROUI, AND L. B. ROMDHANE, *Influential nodes detection in dynamic social networks: A survey*, Expert Systems with Applications, (2020), p. 113642.
- [16] A. A. HAGBERG, D. A. SCHULT, AND P. J. SWART, *Exploring network structure, dynamics, and function using networkx*, in Proceedings of the 7th Python in Science Conference, Pasadena, CA USA, 2008, pp. 11–15.
- [17] D. HAN, D. F. SUN, AND L. ZHANG, *Linear rate convergence of the alternating direction method of multipliers for convex composite programming*, Mathematics of Operations Research, 43 (2018), pp. 622–637.

- [18] I. HIMELBOIM, M. A. SMITH, L. RAINIE, B. SHNEIDERMAN, AND C. ESPINA, *Classifying twitter topic-networks using social network analysis*, Social Media+ Society, 3 (2017), p. 2056305117691545.
- [19] J.-B. HIRIART-URRUTY, J.-J. STRODIOT, AND V. H. NGUYEN, *Generalized Hessian matrix and second-order optimality conditions for problems with  $c^{1,1}$  data*, Applied Mathematics and Optimization, 11 (1984), pp. 43–56.
- [20] J. HONORIO, D. SAMARAS, N. PARAGIOS, R. GOLDSTEIN, AND L. E. ORTIZ, *Sparse and locally constant Gaussian graphical models*, in Advances in Neural Information Processing Systems, 2009, pp. 745–753.
- [21] M. J. HOSSEINI AND S.-I. LEE, *Learning sparse Gaussian graphical models with overlapping blocks*, in Advances in Neural Information Processing Systems, vol. 29, Curran Associates, Inc., 2016, pp. 3808–3816.
- [22] C.-J. HSIEH, M. A. SUSTIK, I. S. DHILLON, AND P. RAVIKUMAR, *Sparse inverse covariance matrix estimation using quadratic approximation*, in Advances in Neural Information Processing Systems, vol. 24, Curran Associates Inc., 2011, pp. 2330–2338.
- [23] C.-J. HSIEH, M. A. SUSTIK, I. S. DHILLON, AND P. RAVIKUMAR, *QUIC: Quadratic approximation for sparse inverse covariance estimation*, Journal of Machine Learning Research, 15 (2014), pp. 2911–2947.
- [24] L. LI AND K.-C. TOH, *An inexact interior point method for  $\ell_1$ -regularized sparse covariance selection*, Mathematical Programming Computation, 2 (2010), pp. 291–315.
- [25] Z. LI, J. BAI, AND W. ZHOU, *Learning Gaussian graphical models using discriminated hub graphical lasso*, in 2018 IEEE International Conference on Acoustics, Speech and Signal Processing (ICASSP), IEEE, 2018, pp. 2471–2475.
- [26] Z. LU, *Smooth optimization approach for sparse covariance selection*, SIAM Journal on Optimization, 19 (2009), pp. 1807–1827.
- [27] Z. MENG, B. ERIKSSON, AND A. HERO, *Learning latent variable Gaussian graphical models*, in Proceedings of the 31st International Conference on Machine Learning, vol. 32, PMLR, 2014, pp. 1269–1277.
- [28] A. J. MOLSTAD AND A. J. ROTHMAN, *Shrinking characteristics of precision matrix estimators*, Biometrika, 105 (2018), pp. 563–574.
- [29] T. NAKAGAKI, M. FUKUDA, S. KIM, AND M. YAMASHITA, *A dual spectral projected gradient method for log-determinant semidefinite problems*, Computational Optimization and Applications, (2020), pp. 33–68.
- [30] F. OZTOPRAK, J. NOCEDAL, S. RENNIE, AND P. A. OLSEN, *Newton-like methods for sparse inverse covariance estimation*, in Advances in Neural Information Processing Systems, vol. 25, Curran Associates, Inc., 2012, pp. 755–763.

- [31] P. RAVIKUMAR, G. RASKUTTI, M. J. WAINWRIGHT, AND B. YU, *Model selection in Gaussian graphical models: High-dimensional consistency of  $\ell_1$ -regularized MLE*, in Proceedings of the 21st International Conference on Neural Information Processing Systems, Curran Associates Inc., 2008, pp. 1329–1336.
- [32] R. T. ROCKAFELLAR, *Convex Analysis*, Princeton University Press, 1970.
- [33] R. T. ROCKAFELLAR, *Augmented Lagrangians and applications of the proximal point algorithm in convex programming*, Mathematics of Operations Research, 1 (1976), pp. 97–116.
- [34] R. T. ROCKAFELLAR AND R. J.-B. WETS, *Variational Analysis*, vol. 317, Springer Science & Business Media, 2009.
- [35] K. SCHEINBERG, S. MA, AND D. GOLDFARB, *Sparse inverse covariance selection via alternating linearization methods*, in Advances in Neural Information Processing Systems, vol. 23, Curran Associates, Inc., 2010, pp. 2101–2109.
- [36] D. W. SOH AND S. TATIKONDA, *Learning unfaithful  $k$ -separable Gaussian graphical models.*, Journal of Machine Learning Research, 20 (2019), pp. 1–30.
- [37] K. M. TAN, P. LONDON, K. MOHAN, S.-I. LEE, M. FAZEL, AND D. WITTEN, *Learning graphical models with hubs*, Journal of Machine Learning Research, 15 (2014), pp. 3297–3331.
- [38] D. A. TARZANAGH AND G. MICHAILIDIS, *Estimation of graphical models through structured norm minimization*, Journal of Machine Learning Research, 18 (2018), pp. 7692–7739.
- [39] C. WANG, D. F. SUN, AND K.-C. TOH, *Solving log-determinant optimization problems by a Newton-CG primal proximal point algorithm*, SIAM Journal on Optimization, 20 (2010), pp. 2994–3013.
- [40] C. WANG AND P. TANG, *A dual semismooth Newton based augmented Lagrangian method for large-scale linearly constrained sparse group square-root lasso problems*, Journal of Scientific Computing, (2023).
- [41] S. YANG, Z. LU, X. SHEN, P. WONKA, AND J. YE, *Fused multiple graphical lasso*, SIAM Journal on Optimization, 25 (2015), pp. 916–943.
- [42] Y.-L. YU, *On decomposing the proximal map*, in Advances in Neural Information Processing Systems, Curran Associates, Inc., 2013, pp. 91–99.
- [43] M. YUAN AND Y. LIN, *Model selection and estimation in the Gaussian graphical model*, Biometrika, 94 (2007), pp. 19–35.
- [44] Y. ZHANG, N. ZHANG, D. F. SUN, AND K.-C. TOH, *An efficient Hessian based algorithm for solving large-scale sparse group lasso problems*, Mathematical Programming, 179 (2020), pp. 223–263.
- [45] ———, *A proximal point dual Newton algorithm for solving group graphical lasso problems*, SIAM Journal on Optimization, 30 (2020), pp. 2197–2220.